

**STUDY ON LOCALIZED AND PROPAGATING
SURFACE PLASMON RESONANCE COUPLING BETWEEN
METAL NANOPARTICLES AND GOLD GRATING THIN FILMS**

CHUTIPARN LERTVACHIRAPAIBOON

**DOCTORAL PROGRAM IN ELECTRICAL AND INFORMATION ENGINEERING
GRADUATE SCHOOL OF SCIENCE AND TECHNOLOGY
NIIGATA UNIVERSITY**

ABSTRACT

This dissertation reports the novel characterization technique based surface plasmon resonance (SPR) spectroscopy. First, solution-based fabrication of gold grating film for use as a SPR sensor chip, gold nanoparticles (AuNPs) grating films were fabricated by imprinting technique. The SPR measurements of this substrate were carried out on a SPR device in the grating-coupling configuration with an excitation source of He-Ne laser ($\lambda = 632.8$ nm) and multimode surface plasmon excitations were observed upon irradiation with white light. From both SPR measurements, imprinted AuNPs grating substrate provided strong SPR excitation signals. The sensitively shift upon organic thin film deposition were observed. Second, transmission surface plasmon resonance (T-SPR) enhancement by localized surface plasmon resonance of metal nanoparticles (*i.e.*, AuNPs and silver nanoparticles (AgNPs)). AuNPs were directly deposited on gold grating surface. The growth mechanism of AuNPs on gold surface was investigated by UV-visible spectroscopy and SPR spectroscopy. The T-SPR results show a possibility of hybrid excitation of localized and propagating surface plasmon. The T-SPR signal enhancement of this hybrid SPR substrate was observed while the multilayer films were deposited on its surface. Furthermore, distance-dependent SPR coupling between metal nanoparticles and gold grating surface was further study. The distance between AgNPs and gold grating surface was controlled by number of bilayers ultrathin film deposition. The distance-dependent T-SPR response of peak position and intensity showed distinctive changes when the intermediate layer was 10 bilayers (~17 nm) thick. This substrate was explored in switchable pH sensor. The T-SPR spectrum sensitively changed as the pH switched from acidic (pH 2) and alkaline (pH 12) conditions by the swelling/shrinking of the polyelectrolyte film between the AgNPs and the gold grating surface.

KEYWORDS: gold nanoparticles, imprinted gold nanoparticles, silver nanoparticle, grating-coupled surface plasmon resonance, transmission surface plasmon resonance

ACKNOWLEDGMENTS

I would like to express my sincere gratitude to my thesis advisors, Associate Professor Dr. Akira Baba and Associate Professor Dr. Sanong Ekgasit for invaluable guidance and suggestions throughout this work.

I wish to express my grateful thank to Professor Dr. Futao Kaneko, Professor Dr. Keizo Kato, Professor Dr. Kazunari Shinbo, and Associate Professor Chuchaat Thammacharoen from Chulalongkorn University for their valuable advice.

Warmest thanks to my friend, my colleagues and organization: Center for Transdisciplinary Research, Niigata University, and all good friends for suggestion and spiritual supports throughout this research.

The financial support from The “Global Circus” Program of Niigata University supported by the Ministry of Education, Culture, Sports, Science and Technology.

Above all, I am profoundly grateful to my parents and endearing family for all their loaves, understanding, support, and encouragement during the whole preiod of my study.

CONTENTS

	Page
ABSTRACT.....	ii
ACKNOWLEDGMENTS.....	iii
CONTENTS.....	iv
LIST OF FIGURE.....	vi
LIST OF ABBREVIATIONS.....	ix
CHAPTER I INTRODUCTION.....	1
1.1 RESEARCH BACKGROUND AND RATIONALE.....	1
1.1.1 Transmission surface plasmon resonance (T-SPR).....	1
1.1.2 Gold nanoparticles synthesis and their applications.....	2
1.1.3 Localized surface plasmon resonance (LSPR).....	4
1.1.4 Hybrid excitation of localized and propagating surface plasmons.....	6
1.2 OBJECTIVES.....	7
1.3 SCOPE OF THE DISSERTATION.....	8
CHAPER II Solution-Based Fabrication of Gold Grating Film for Use as a Surface Plasmon Resonance Sensor Chip.....	13
ABSTRACT.....	14
INTRODUCTION.....	14
EXPERIMENTAL.....	15
RESULTS AND DISCUSSION.....	18
CONDLUSIONS.....	23
REFERENCES.....	24
CHAPER III Transmission Surface Plasmon Resonance Signal Enhancement via Growth of Gold Nanoparticles on a Gold Grating Surface.....	28
ABSTRACT.....	29
INTRODUCTION.....	29
EXPERIMENTAL.....	30
RESULTS AND DISCUSSION.....	33

	Page
CONDLUSIONS.....	41
REFERENCES.....	42
CHAPER IV Distance-Dependent Surface Plasmon Resonance Coupling between a Gold Grating Surface and Silver Nanoparticles.....	45
ABSTRACT.....	46
INTRODUCTION.....	46
EXPERIMENTAL.....	48
SYNTHESIS OF SILVER NANOPARTICLES.....	48
LAYER-BY-LAYER ADSORPTION.....	48
DEPOSITION OF SILVER NANOPARTICLES.....	49
T-SPR SPECTROSCOPY.....	49
PH-SWICHABLE SWALLING/SHRINKING INVESTIGATED BY T-SPR SPECTROSCOPY.....	49
RESULTS AND DISCUSSION.....	50
CONDLUSIONS.....	59
REFERENCES.....	59
CHAPER V CONCLUSIONS.....	62
SUGGESTIONS FOR FUTURE WORK.....	63
APPENDICES.....	64
APPENDIX A.....	65
APPENDIX B.....	69
APPENDIX C.....	71
APPENDIX D.....	75
VITAE.....	78

LIST OF FIGURE

Figure	Page
CHAPTER I INTRODUCTION	
1. Gold nanohole arrays (a), gold grating patterns (b) and their corresponding T-SPR signal	1
2. Assay of milk samples with and without common interfering substances. The sample consisting of (a) 1% milk, (b) 0.1% milk, (c) 0.1% milk with 1% starch, (d) with 0.1 M lactose, (e) with 1% sugar, (f) with 0.01 M melamine, and (g) with 0.1 M NaCl.....	3
3. Photographic images of AuNPs in the presence of 0.01% dedecyltrimethylammonium bromide (DTAB) (a) and 0.01 μ L of octanethiol in the hexane phase (b). SERS and Raman spectra of crystal violet drop-casted film (black line), on octanethiol-mediated gold film (blue line) and on DTAB-mediated gold film (red line).....	4
4. Localized surface plasmon resonance (LSPR).....	5
5. The LSPR spectra of gold nanoparticles at difference sizes.....	6
6. The LSPR spectra of silver nanobars (a) and nanorice (b).....	6
7. Schematic drawing of nanoparticle-enhanced diffraction gratings (NEDG) experimental setup (a) and time-dependent NEDG signal curves for detection of target DNA at concentrations ranging from 10 to 100 fM (b).....	7
 CHAPER II Solution-Based Fabrication of Gold Grating Film for Use as a Surface Plasmon Resonance Sensor Chip	
1. Schematic of the synthesis of AuNP (a) and imprinting of AuNP on a grating pattern (b)...	17
2. LSPR excitation of AuNP (a) and histogram of the size and size distribution of AuNPs (b)	18
3. AFM images of AuNP films before (a) and after (b) annealing.....	19
4. AFM image (a) and topology profile (b) of annealed imprinted AuNP grating pattern.....	20
5. Surface plasmon reflectivity curves of imprinted AuNP grating substrate (a) and evaporated gold grating substrate (b).....	21
6. SPR reflectivity curves of imprinted AuNP at a fixed incident angle from 35° to 70° as a function of wavelength (a) and plotted dots obtained from experimental dip angles and calculated SP dispersion (b).....	22
7. SPR angular curves of imprinted AuNP substrate before and after the deposition of LbL ultrathin film obtained using a He-Ne laser (a) and white light excitation (b).....	23

Figure	Page
CHAPTER III Transmission Surface Plasmon Resonance Signal Enhancement via Growth of Gold Nanoparticles on a Gold Grating Surface	
1. Experimental procedure for growing gold nanoparticles on a gold-coated grating surface....	31
2. Schematic diagram of the T-SPR instrumental setup.....	32
3. Schematic drawing of Au grating film with gold (thickness 50 nm) polycarbonate grating structure (grating pitch, $\Lambda = 740$ nm) (a). Electric field of Au grating film (b), AuNPs (small particles)/Au grating film (c) and AuNPs (large particles)/Au grating film (d) in the environment of water and the enlargement of schematic drawing which corresponds with AuNPs on the gold grating used in our experiments.....	34
4. UV-visible spectra of AuNPs grown on Au film substrate, obtained at various incubation times and the inset spectrum shows the enlargement of UV-visible spectrum of AuNPs grown on Au film substrate at 4 h incubation.....	35
5. SPR experimental and fitted SPR curves of AuNPs grown on Au film substrate obtained at various incubation times (a) (The inset shows the SPR dip angle as a function of incubation time). Plot of Au film thickness as a function of incubation time (b).....	37
6. AFM image of bare Au grating surface (a), AuNPs/Au grating surfaces with incubation time of 4 (b), 6 (c), and 8 h (d). The corresponding schematic drawing of gold nanoparticles on the gold grating at the given incubation time is proposed.....	38
7. T-SPR spectra with the angle of incidence of $25 - 40^\circ$ of the bare Au grating substrate (a) and that of AuNPs/Au grating substrate with 4 h incubation (b). The angle of incident is indicated above the corresponding spectrum.....	39
8. T-SPR spectra of bilayers fabricated on substrate monitored at the angle of incidence 35° : bare Au grating substrate (a), AuNPs/Au grating substrate with 4 h incubation (b), and plots of changes in the T-SPR intensity as a function of the number of bilayers (c) on bare Au grating substrate (open square, black), AuNPs/Au grating substrate with 4 h (filled square, red), 6 h (open circle, green), and 8 h (filled circle, blue) incubations.....	40
CHAPTER IV Distance-Dependent Surface Plasmon Resonance Coupling between a Gold Grating Surface and Silver Nanoparticles	
1. Schematic diagram of the sample structure.....	50
2. LSPR excitation of AgNPs at various distances from a BK7 glass slide.....	51

Figure	Page
3. The T-SPR spectra of the gold grating substrate ($\Lambda = 740$ nm) at various angles (a). The T-SPR spectrum of an ultrathin film on the gold grating substrate was monitored at an incidence angle of 35° (b). The inset plot is the change in the T-SPR intensity as a function of the number of bilayers.....	52
4. T-SPR spectra of films with 10-bilayer (a) and 30-bilayer (b) spacers, respectively. Plot of the T-SPR responses showing the shift in peak position and the increase in T-SPR intensity as a function of the number of bilayers spacers.....	54
5. Absorption spectrum of AgNPs on a gold grating with an intermediate layer (10 bilayers of PDADMAC/PSS) (a) and without an intermediate layer (b) at an angle of incidence of 35° under s-polarization. The inset spectrum shows the development of the T-SPR spectrum when the number of AgNPs layers was increased.....	56
6. T-SPR spectrum of a [(PAH/PSS) ₁₀ + (PAH/AgNPs) ₅] film at pH 2 (red line) and at pH 12 (blue line) (a). Schematic diagram of swelling and shrinking as the PAH layers were protonated (pH 2) and deprotonated (pH 12), respectively (b). Kinetic curve of the film when the pH was switched between 2 and 12; the switch was repeated three times (c).....	58

LIST OF ABBREVIATIONS

SPR	Surface plasmon resonance
LSPR	Localized surface plasmon resonance
T-SPR	Transmission surface plasmon resonance
AuNPs	Gold nanoparticles
AgNPs	Silver nanoparticles
AFM	Atomic force microscope
FDTD	Finit-difference time-domain
PEDOT:PSS	poly(3,4-ethylenedioxythiophene):poly(styrenesulfonate)
TMPyP	5, 10, 15, 20-tetrakis (1-methyl-4-pyridinio) porphyrin tetra (<i>p</i> -toluenesulfonate)
SCC	and sodium copper chlorophyllin
APS	3-aminopropyltriethoxysilane
MPS	3-mercapto-1-propanesulfonic acid sodium salt
PDADMAC	poly(diallyldimethylammonium chloride)
PSS	poly(sodium 4-styrenesulfonate)
PAH	poly(allylamine hydrochloride)

CHAPTER I

INTRODUCTION

1.1 RESEARCH BACKGROUND AND RATIONALE

1.1.1 Transmission surface plasmon resonance (T-SPR)

Surface plasmon resonance (SPR) on a diffraction grating is widely used to characterize and study ultrathin films, analytical surface binding, biomolecules immobilization, and surface kinetic processes [1, 2]. Various types of grating structures can be used for SPR excitation. The flexibility and simplicity of the system make grating-based SPR a research topic of significant interest [1-10]. SPR excitation has recently been shown to enhance light transmission through nanostructures such as hole arrays [11, 12] and grating patterns [8-10] and, of particular interest, through grating substrates of commercial digital versatile disc-recordables (DVD-Rs) coated with thin gold films [6, 7]. Significantly, transmission SPR (T-SPR) spectra of light transmitted through such a gold grating substrate show strong, narrow peaks in the visible light region. The T-SPR wavelength depends on the grating pitch and the angle of incidence [6, 7]. Figure 1a and 1b show gold nanohole arrays and gold grating patterns, respectively.

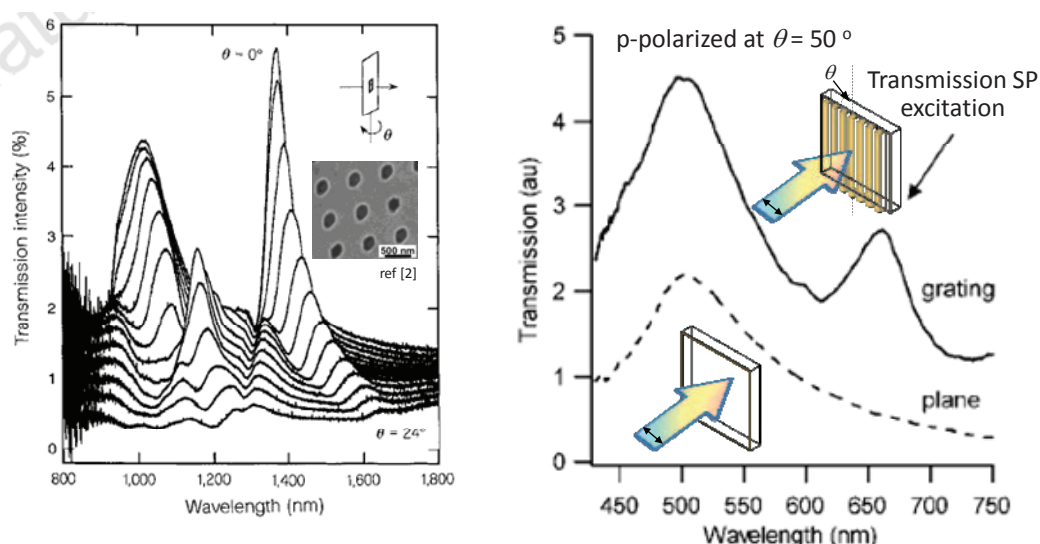


Figure 1 Gold nanohole arrays (a), gold grating patterns (b) and their corresponding T-SPR signal [7, 11].

Recently, diffraction-based surface enhanced transmission was reported that the ± 1 diffracted orders from the gold grating film were detected [13]. The optical transmission is based on the decoupling of surface plasmons which is excited and confined at the surface of metals. Hence, the T-SPR spectrum is highly sensitive to the local refractive index near a metal/dielectric interface, making T-SPR spectroscopy a useful technique for optical sensing applications. The sensitivity depends especially on the surface structures for the coupling of near field SP excitations and decoupling to far field freely propagating light [14-16]. However, to our knowledge, there is no report to further enhance the T-SPR signals with the modification of the nanostructured surfaces.

1.1.2 Gold nanoparticles synthesis and their applications

Gold nanoparticles (AuNPs) are of considerable interest in scientific research and industrial applications because of their unique and unusual size dependent properties associated with their large surface area to volume ratio. AuNPs have been employed in various applications: they have been used as catalysts, surface-enhanced spectroscopy, and sensors [17-19]. Since AuNPs express surface plasmon (SP) excitation at the vicinity of their surface [20,21], surface plasmon resonance (SPR) sensors based on AuNPs have been widely used for detection of proteins [22], antibodies [23], and nucleic acids [24]. Field enhancement at different wavelengths associated with SPR is also exploited in many surface analytical techniques such as surface-enhanced Raman spectroscopy (SERS) [18,25,26], surface-enhanced infrared absorption spectroscopy (SEIRA) [26,27], and surface-enhanced fluorescence spectroscopy [28].

The most referred method for gold nanoparticles synthesis was proposed in 1953, AuNPs were synthesized by Turkevich and co-workers [29]. Aurochloric acid was reduced by sodium citrate. The sphere-shaped of AuNPs with the average size of 20 nm in diameter was a product. At that time, the synthesis product was called as ‘colloidal gold’. Interestingly, this study showed that seed of gold particles could induce gold ion in the system to form gold nanoparticles

In 2007, High concentration of AuNPs was synthesized by Guo and Wang [30]. HAuCl_4 was mixed with poly(*N*-vinyl-2-pyrrolidone) (PVP) and *o*-diaminobenzene was used as a reducing agent. The reaction was performed at room temperature for several hours. The particles were controlled from nanoscale to micro scale by changing the ratio of HAuCl_4 and

PVP concentration. The highest concentration, which they could synthesis was 2,000 ppm, but at this concentration, the size of gold particles were in the size of micrometer size. The nanosize of gold particles were observed when the concentration of colloid was under 100 ppm.

In 2012, the green technology approach was the topic of interest, AuNPs synthesis using starch as the reducing agent and stabilizer was reported by Pienpinijtham and co-workers [31]. The size of the gold particles can be selectively tuned from nanometer to submicrometer regimes with narrow size distribution through pH adjustment of the solution. Under alkaline condition, reducing efficiency of starch was enhanced by the concomitant generation of reducing species (aldehyde or α -hydroxy ketone). The resulting AuNPs was very stable, which can be kept over 4 months without aggregation, or any significant changes.

Mostly, AuNPs could be used in sensor applications. In 2012, Naked eye colorimetric quantification of protein in milk using AuNPs was investigated by Vantasin and co-worker [32]. AuNPs were aggregated in contact of hydrochloric acid. The degree of aggregation could be reduced in the presence of milk protein, depending on protein concentration. The sensitive range of assay could be adjusted by concentration of AuNPs as the assay sensitive in 2.93×10^{-1} to 2.93×10^{-2} mg/mL protein range for 1,000 ppm AuNPs and sensitive in 2.93×10^{-2} to 2.93×10^{-3} mg/mL protein range for 200 ppm AuNPs. The result could be easily observed by naked-eye sensing as the color appeared red for higher protein concentration and appeared violet-blue for lower protein concentration in the sensitive range.

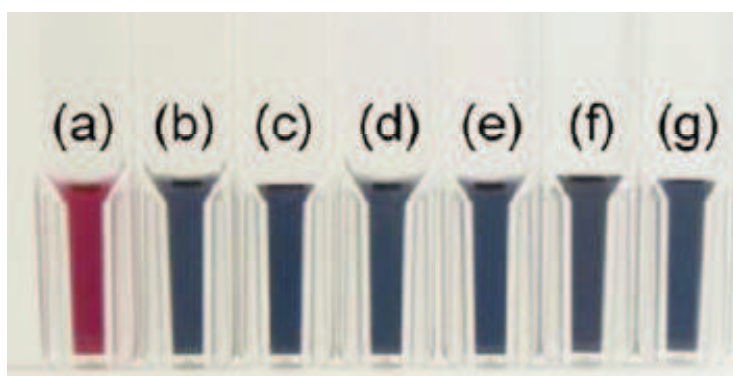


Figure 2 Assay of milk samples with and without common interfering substances. The sample consisting of (a) 1% milk, (b) 0.1% milk, (c) 0.1% milk with 1% starch, (d) with 0.1 M lactose, (e) with 1% sugar, (f) with 0.01 M melamine, and (g) with 0.1 M NaCl [32].

Recently, surface enhanced Raman spectroscopy (SERS) has become a powerful technique for characterization of trace samples. AuNPs is a one of metal nanoparticles which have been developed for SERS due to their stability and strong signal in SERS technique. The assembled AuNPs film was formed by Langmuir-Blodgett (LB) method for using as a SERS substrate [33]. The SERS enhancement of this substrate was approximately 1.2×10^6 using crystal violet as a Raman dye. High reproducibility and stability could be obtained by this technique.

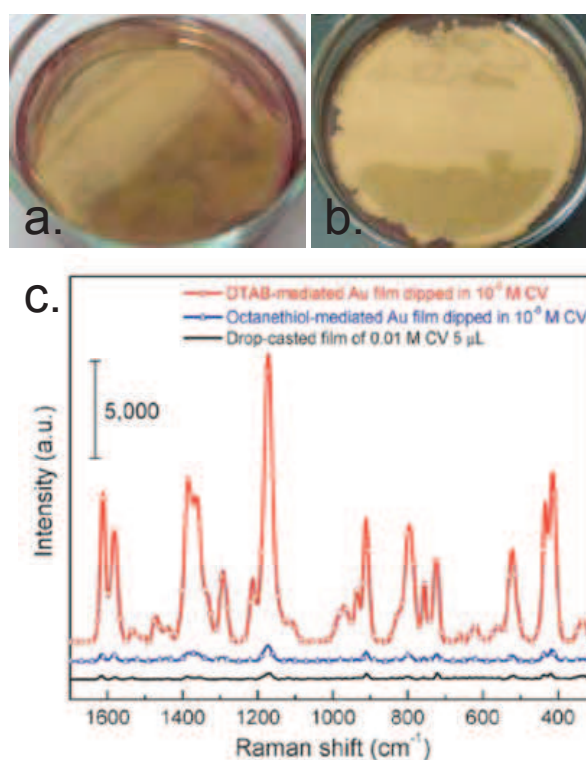


Figure 3 Photographic images of AuNPs in in the presence of 0.01% dedecyltrimethylammonium bromide (DTAB) (a) and 0.01 μ L of octanethiol in the hexane phase (b). SERS and Raman spectra of crystal violet drop-casted film (black line), on octanethiol-mediated gold film (blue line) and on DTAB-mediated gold film (red line) [33].

1.1.3 Localized surface plasmon resonance (LSPR)

Localized surface plasmon resonance is the oscillated electron of metal nanostructures coupled to the same as energy of external electromagnetic filed, as shown in Figure 2. External electromagnetic filed is transformed to thermal energy and radiated energy to any

direction, which is known as an absorption and scattering phenomenon, respectively. Sum of absorption and scattering is called as extinction. Therefore, the definition of extinction is the total electromagnetic field crossing the surface of the particles as a function of the irradiance of the incident light [20].

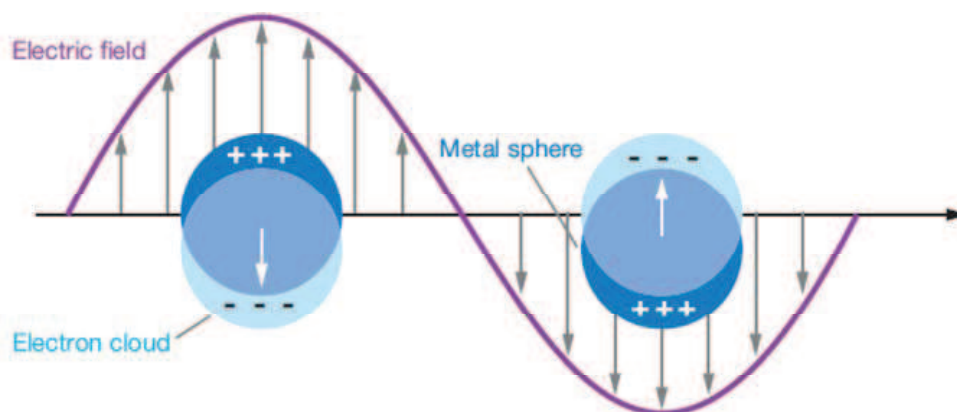


Figure 4 Localized surface plasmon resonance (LSPR) [20]

LSPR frequency depends on the shape, size of metal particles with respect to oscillation of electron on the metal particles surface. The larger particle has longer distance for the electron oscillation, LSPR frequency shows at the lower frequency or longer wavelength. For non-spherical and very large metal particles, electron on the metal nanoparticles surface can oscillate through different direction, resulting in several oscillation frequencies. Figure 5 show the LSPR spectra of AuNPs at different sizes. Figure 6 shows the LSPR spectra of silver nanobars (a) and nanorice (b). As shown in figure 6, silver nanobars and nanorice exhibit two plasmon resonance peaks in visible and near-infrared regions which are sensitive to aspect ratio of particles [35].

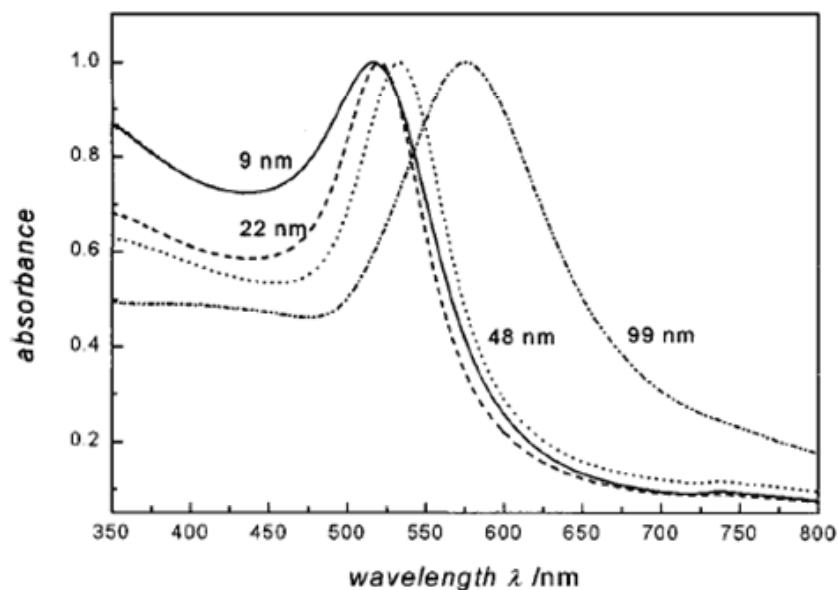


Figure 5 The LSPR spectra of gold nanoparticles at difference sizes [34].

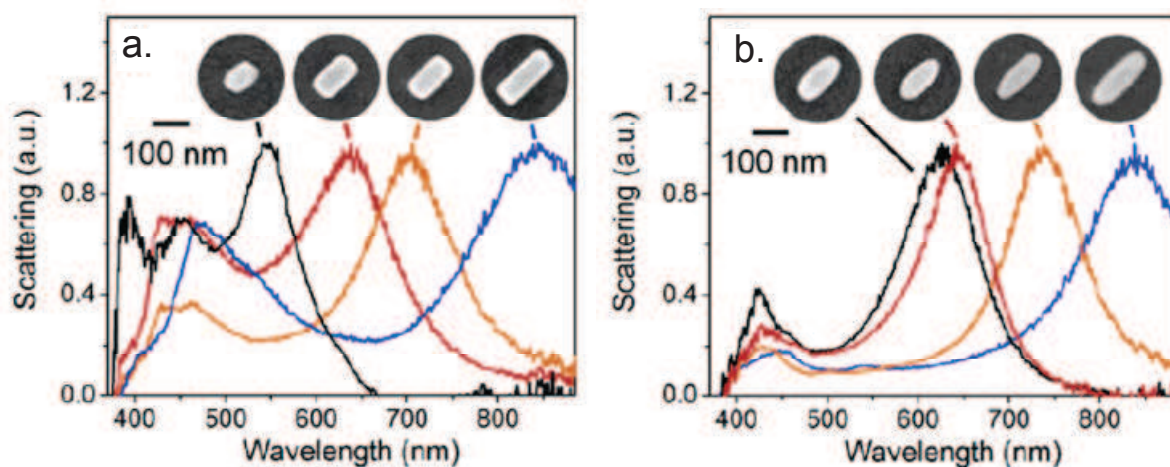


Figure 6 The LSPR spectra of silver nanobars (a) and nanorice (b) [35].

1.1.4 Hybrid excitation of localized and propagating surface plasmons

In the past decade, the classical gold film with the thickness of 50 nm was still exploited in SPR sensors. The improvement of sensitivity have been achieved with excitation further in integrating of SPR sensor to a diffraction grating [36,37], long-range surface plasmons (LRSP) [38], Fourier transform-infrared (FT-IR) spectroscopy [39], and micro/nanopattern of gold films [11,12,40,41]. Enhanced sensitivity of SPR sensing was

reported by a hybrid material of gold grating pattern and AuNPs, observing large changes in diffraction efficiency at the SPR wavelength. Femtomolar levels of DNA detection in a sandwich assay was reported by Wark and co-workers [41]. T-SPR spectroscopy is one of SPR technique, which is useful for optical sensing application. Recently, T-SPR signal enhancement by synthesis of AuNPs on gold grating surface was reported [37]. The T-SPR intensity of this hybrid material showed strong spectrum and shift beyond that of conventional 50 nm-thick gold grating film. As the localized surface plasmon from metal nanoparticles facilitate the coupling/decoupling of surface plasmons and may also excite surface plasmon, further enhancement of this hybrid material could be exhibited.

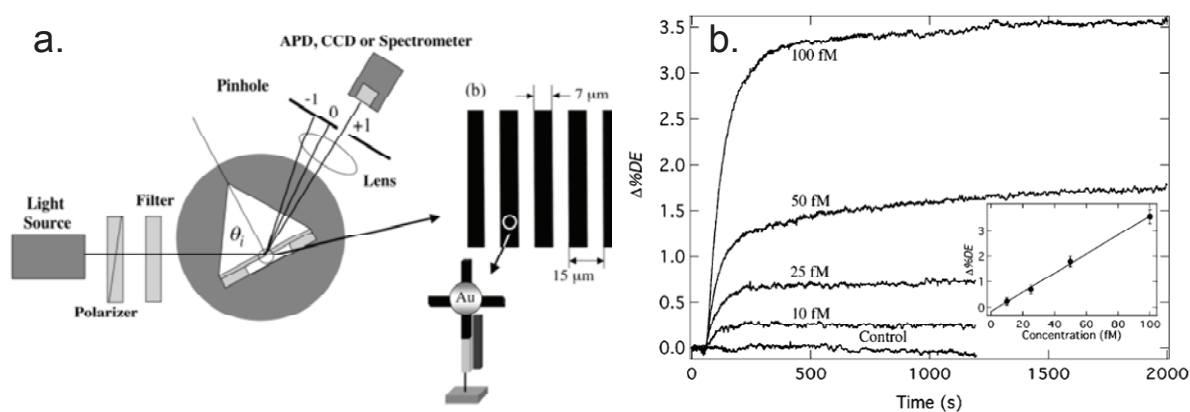


Figure 7 Schematic drawing of nanoparticle-enhanced diffraction gratings (NEDG) experimental setup (a) and time-dependent NEDG signal curves for detection of target DNA at concentrations ranging from 10 to 100 fM (b) [41].

1.2 OBJECTIVES

Due to the interestedness of SPR technique and its signal enhancement by LSPR of metal nanoparticles as discussed above, novel hybrid material for enhancement of SPR signal are necessary to be developed, and the synthesized metal nanoparticles methods were adjusted to fit with several kind of SPR techniques. Therefore, major aims of this thesis are:

1. To synthesize high concentration of gold nanoparticles for use as a surface plasmon resonance sensor chip.

2. To study the growth mechanism of gold nanoparticles on gold surface and explore the enhancement of transmission surface plasmon resonance signal by growth of gold nanoparticles on a gold grating substrate.
3. To study the distance-dependent surface plasmon resonance coupling between a gold grating surface and silver nanoparticles.

1.3 SCOPE OF THE DISSERTATION

This dissertation mainly focused on synthesis of gold and silver nanoparticles using chemical reduction method and exploitation in SPR sensor chip and also enhanced T-SPR signal. The detail investigation for using AuNPs as SPR sensor chip was deeply investigated. The SPR measurements were carried out on an SPR device in the grating-coupling configuration with a He-Ne laser as the excitation source and multimode SPR excitations were observed upon irradiation with white light. The surface plasmon dispersion branches were calculated to obtain the diffraction order in investigated region. For T-SPR signal enhancement by growth of AuNPs on gold grating surface, the T-SPR signal enhancement of this hybrid material was investigated compared with the regular gold grating film. The growth mechanism of AuNPs on gold film surface was deeply studied using UV-visible spectroscopy, prism-coupled SPR spectroscopy, and atomic force microscopy. Furthermore, the deposition of silver nanoparticles (AgNPs) on gold grating surface was also explored to prove T-SPR signal enhancement by LSPR of metal nanoparticles. The distance-dependent SPR coupling between gold grating surface and AgNPs were further investigated. The intermediate layers were controlled by the thickness of ultrathin film to obtain the optimum distance which provided the greatest coupling of electric field enhancement. Therefore, three work chapters are included as follows:

- 1. Solution-Based Fabrication of Gold Grating Film for Use as a Surface Plasmon Resonance Sensor Chip**
- 2. Transmission Surface Plasmon Resonance Signal Enhancement via Growth of Gold Nanoparticles on a Gold Grating Surface**
- 3. Distance-Dependent Surface Plasmon Resonance Coupling between a Gold Grating Surface and Silver Nanoparticles**

REFERENCES

1. W. Knoll, Interfaces and thin films as seen by bound electromagnetic wave. *Annu. Rev. Phys. Chem.* 49 (1998) 569-638.
2. J. Homola, I. Koudela, S.S. Yee, Surface plasmon resonance sensors based on diffraction gratings and prism coplers: sensitivity comparison, *Sens. Actuators. B* 54 (1999) 16-24.
3. A. Baba, K. Kanda, T. Ohno, Y. Ohdaira, K. Shinbo, K. Kato, F. Kaneko, Multimode surface plasmon excitations on organic thin film/metallic diffraction grating, *Jpn. J. Appl. Phys.* 49 (2010) 01AE02-1-01AE02-4.
4. A. Baba, N. Aoki, K. Shinbo, K. Kato, F. Kaneko, Grating-coupled surface plasmon enhanced short-circuit current in organic thin-film photovoltaic cells, *ACS Appl. Mater. Interfaces.* 3 (2011) 2080-2084.
5. A. Baba, K. Wakatsuki, K. Shinbo, K. Kato, F. Kaneko, Increased short-circuit current in grating-coupled surface plasmon resonance field-enhanced dye-sensitized solar cells, *J. Mater. Chem.* 21 (2011) 16436-16441.
6. B.K. Singh, A.C. Hillier, Surface plasmon resonance imaging of biomolecular interactions on a grating-based sensor array, *Anal. Chem.* 78 (2006) 2009-2018.
7. B.K. Singh, A.C. Hillier, Surface plasmon resonance enhanced transmission of light through gold-coated diffraction gratings, *Anal. Chem.* 80 (2008) 3803-3810.
8. Z.C. Xu, B. Dong, J. Xue, R. Yang, B.R. Lu, S. Deng, Z.F. Li, W. Lu, Y. Chen, E. Huq, X.P. Qu, R. Liu, Surface plasmon polariton coupling induced transmission of subwavelength metallic grating with waveguide layer, *Microelectron. Eng.* 87 (2010) 1297-1299.
9. B. Turker, H. Guner, S. Ayas, O.O. Ekiz, H. Acar, M.O. Guler, A. Dâna, Grating coupler integrated photodiodes for plasmon resonance based sensing, *Lab Chip* 11 (2010) 282-287.
10. W.H. Yeh, J. Kleingartner, A.C. Hillier, Wavelength tunable surface plasmon resonance-enhanced optical transmission through a chirped diffraction grating, *Anal. Chem.* 82 (2010) 4988-4993.
11. T.W. Ebbesen, H.J. Lezec, H.F. Ghaemi, T. Thio, P.A. Wolff, Extraordinary optical transmission through sub-wavelength hole arrays, *Nature* 391 (1998) 667-669.

12. A.G. Brolo, R. Gordon, B. Leathem, K.L. Kavanagh, Surface plasmon sensor based on the enhanced light transmission through array of nanoholes in gold films, *Langmuir* 20 (2004) 4813-4815.
13. W.H. Yeh, J.W. Petefish, A.C. Hillier, Diffraction-based tracking of surface plasmon resonance enhanced transmission through a gold-coated grating, *Anal. Chem.* 83 (2011) 6047-6053.
14. H. Liu, P. Lalanne, Microscopic theory of the extraordinary optical transmission, *Nature*, 452 (2008) 728-731.
15. E. Devaux, T.W. Ebbesen, J.C. Weeber, A. Dereux, Launching and decoupling surface plasmon via micro-grating, *Appl. Phys. Lett.*, 83 (2003) 4936-4938.
16. U. Scheröter, D. Heitmann, Surface-plasmon-enhanced transmission through metallic gratings. *Phys. Rev. B*, 58 (1998) 15419-15421.
17. H. Wu, L. Wang, J. Zhange, Z. Shen, J. Zhao, Catalytic oxidation of benzene, toluene and *p*-xylene over colloidal gold supported on zinc oxide catalyst, *Catal. Commun.* 12 (2011) 859-865.
18. P. Pienpinijitham, X.X. Han, S. Ekgasit, and Y. Ozaki, Highly Sensitive and Selective Determination of Iodide and Thiocyanate Concentrations Using Surface-Enhance Raman Scattering of Starch-Reduced Gold Nanoparticles, *Anal. Chem.* 83 (2011) 3655–3662.
19. N. Ciofffi, L. Colaianni, E. Ieva, R. Pilolli, N. Ditaranto, M.D. Angione, S. Cotrone, K. Buchholt, A.L. Spetz, L. Sabbatini, and L. Torsi, Electrocynthesis and characterization of gold nanoparticles for electronic capacitance sensing of pollutants, *Electrochim Acta* 56 (2011) 3713-3720.
20. J. Zhao, X. Zhnaga, C.R. Yonzon, A.J. Haes, R.P. Van Duyne, Localized surface plasmon resonance biosensors, *Nanomedicine* 1 (2006) 219-228.
21. K. A. Willets, R.P. Van Duyne, Localized surface plasmon resonance spectroscopy and sensing, *Annu. Rev. Phys. Chem.* 58 (2007) 267-297.
22. J. Deka, A. Paul, A. Chattopadhyay, Sensitive Protein Assay with Distinction of Conformations Based on Visible Absorption Changes of Citrate-Stabilized Gold Nanoparticles, *J. Phys. Chem. C*. 113 (2009) 6936-6947.
23. G. Liu, J. Liu, T.P. Davis, J.J. Gooding, Electrochemical impedance immunosensor based on gold nanoparticles and aryl diazonium salt functionalized gold electrodes for the detection of antibody, *Biosens. Bioelectron.* 26 (2011) 3660-3665.

24. A. Jyoti, P. Pandey, S.P. Singh, S.K. Jain, R. Shanker, Colorimetric Detection of Nucleic Acid Signature of Shiga Toxin Producing Escherichia coli Using Gold Nanoparticles, *J. Nanosci. Nanotechnol.* 10 (2010) 4154-4158.
25. L. Zhange, L. Chen, H. Liu, Y. Hou, A. Hirata, T. Fujita, M. Chen, Effect of Residual Silver on Surface-Enhanced Raman Scattering Dealloyed Nanoporous Gold, *J. Phys. Chem. C* 115 (2011) 19583-19587.
26. M. Baia, F. Toderas, L. Baia, D. Maniu, S. Astilean, Multilayer Structure of Self-Assembled Gold Nanoparticles SERS and SEIRA Substrate, *ChemPhysChem* 10 (2009) 1106-1111.
27. N. Wisitruangsakul, I. Zebger, K.H. Ly, D.H. Murgida., S. Ekgasit, P. Hildebrandt, Redox-linked protein dynamic of Cytochrome C probe by time-resolved surface enhanced infrared absorption spectroscopy, *Phys. Chem. Chem. Phys* 10 (2008) 5276-5286.
28. L. Shange, J. Yin, J. Li, L. Jin, S. Dong, Gold nanoparticle-based near-infrared fluorescent detection of biological thiols in human plasma, *Biosens. Bioelectron.* 25 (2009) 269-274.
29. J. Turkevich, P.C. Stevenson, J. Hillier, The formation of colloidal gold, *J. Phys. Chem.* 57 (1953) 670-673.
30. S. Guo, E. Wang, One-pot, high-yield synthesis of size-controlled gold particles with narrow size distribution, *Inorg. Chem.* 46 (2007) 6740-6743.
31. P. Pienpinijtham, C. Thammacharoen, S. Ekgasit, Green synthesis of size controllable and uniform gold nanospheres using alkaline degradation intermediates of soluble starch as reducing agent and stabilizer, *Macromol. Res.* 20 (2012) 1281-1288.
32. S. Vantasin, P. Pienpinijtham, K. Wongravee, C. Thammacharoen, S. Ekgasit, Naked eye colorimetric quantification of protein content in milk using starch-stabilized gold nanoparticles, *Sens. Actuators B* 177 (2013) 131-137.
33. P. Pienpinijtham, X.X. Han, S. Ekgasit, Y. Ozaki, An ionic surfactant-mediated Langmuir-Blodgett method to construct gold nanoparticles films for surface-enhanced Raman scattering, *Phys. Chem. Chem. Phys.* 14 (2012) 10132-10139.
34. S. Link, M.A. El-sayed, Size and temperature dependence of the plasmon absorption of colloidal gold nanoparticles, *J. Phys. Chem. B*, 103 (1999) 4212-4217.
35. B.J. Wiley, Y. Chen, J.M. McLellan, Y. Xiong, Z. Li, D. Ginger, Y. Xia, Synthesis and optical properties of silver nanobars and nanorice, *Nano. Lett.* 7 (2007) 1032-1036.

36. F. Yu, S.J. Tian, D.F. Yao, W. Knoll, Surface Plasmon Enhanced Diffraction for Label-Free Biosensing, *Anal. Chem.* 76 (2004) 3530–3535.
37. C. Lertvachirapaiboon, C. Supunyabut, A. Baba, S. Ekgasit, C. Thammacharoen, K. Shinbo, K. Kato, F. Kaneko, Transmission surface plasmon resonance signal enhancement via growth of gold nanoparticles on a gold grating surface, *Plasmonics* 8 (2013) 369-375.
38. G.G. Nenninger, P. Tobiska, J. Homola, S.S. Yee, Long-range surface plasmons for high-resolution surface plasmon resonance sensors, *Sens. Actuators B* 74 (2001) 145–151.
39. N. Menegazzo, L.L. Kegel, Y.C. Kim, K.S. Booksh, Characterization of a Variable Angle Reflection Fourier Transform Infrared Accessory Modified for Surface Plasmon Resonance Spectroscopy, *Appl. Spectrosc.* 64 (2010) 1181–1186.
40. L.S. Live, O.R. Bolduc, J.F. Masson, Propagating Surface Plasmon Resonance on Microhole, *Arrays. Anal. Chem.* 82 (2010) 3780–3787.
41. A.W. Wark, H.J. Lee, A.J. Qavi, R.M. Corn, Nanoparticles-enhanced diffraction grating for ultrasensitive surface plasmon biosensing, *Anal. Chem.* 79 (2007) 6697–6701.

CHAPTER II

Solution-Based Fabrication of Gold Grating Film for Use as a Surface Plasmon Resonance Sensor Chip

Chutiparn Lertvachirapaiboon^{1,2}, Ryosuke Yamazaki¹, Prompong Pienpinijtham²,
Akira Baba^{1*}, Sanong Ekgasit^{2*}, Chuchaat Thammacharoen², Kazunari Shinbo¹,
Keizo Kato¹, and Futao Kaneko¹

¹ Graduate School of Science and Technology and Center for Transdisciplinary
Research, Niigata University, 8050 Ikarashi 2-nocho, Nishi-ku, Niigata 950-2181,
JAPAN.

² Sensor Research Unit, Department of Chemistry, Faculty of Science,
Chulalongkorn University, 254 Phayathai Rd., Patumwan, Bangkok 10330,
THAILAND.

**This article has been published in Journal: Sensors and Actuators B:
Chemical. Volume: 173, Pages: 316-321, Year: 2012.**

ABSTRACT

Imprinted solution-processible gold nanoparticle (AuNP) grating films were fabricated for use as a grating-coupled surface plasmon resonance (SPR) excitation substrate. The imprinted AuNP grating pattern, which consists of a 1.72 μm grating pitch, was fabricated on flat glass substrates by imprinting AuNP on silicon grating templates. In this study, the SPR measurements were carried out on an SPR device in the grating-coupling configuration with a He-Ne laser ($\lambda = 632.8 \text{ nm}$) as the excitation source, and multimode surface plasmon excitations were observed upon irradiation with white light. SPR excitation of our substrate was observed at the incident angle of 47.1° . For SPR measurements using white light irradiation, multimode surface plasmon excitation resulting from several diffraction orders was observed in the wavelength region of 500–850 nm. The surface plasmon dispersion branches were calculated to obtain the diffraction order in this region. SPR excitation of the imprinted AuNP grating substrate was further studied by fabrication of a Layer-by-Layer (LbL) ultrathin film of iron containing bis(terpyridine) polymer (Fe(II)-BTP) and poly(3,4-ethylenedioxythiophene):poly(styrenesulfonate) (PEDOT:PSS). A shift of the SPR excitation spectrum was observed when the ultrathin film was deposited on the imprinted AuNP grating surface. Thus, this substrate should be a useful SPR substrate in a variety of applications such as photoelectric conversions and sensors.

INTRODUCTION

Gold nanoparticles (AuNP) are of considerable interest in scientific research and industrial applications because of their unique and unusual size dependent properties associated with their large surface area to volume ratio. AuNP have been employed in various applications: they have been used as catalysts [1], surface-enhanced spectroscopy [2], and sensors [3]. Since AuNP express surface plasmon (SP) excitation at the vicinity of their surface [4,5], surface plasmon resonance (SPR) sensors based on AuNP have been widely used for detection of proteins [6], antibodies [7], and nucleic acids [8]. Field enhancement at different wavelengths associated with SPR is also exploited in many surface analytical techniques such as surface-enhanced Raman spectroscopy (SERS) [2,9,10], surface-enhanced infrared absorption spectroscopy (SEIRA) [10,11], and surface-enhanced fluorescence spectroscopy [12].

Grating-coupled SPR spectroscopy has been widely used for the characterization and study of ultrathin films, analytical surface binding, biomolecule immobilization, and surface kinetic processes [13,14]. One major advantage of using the grating-coupling excitation method is that a prism is not necessary. Hence, inexpensive and disposable plastics can be used as substrates, allowing for more flexible configurations [15-19]. In 2006, Zhang et al. reported a method for fabricating a periodic array of gold nanowire forms by spin-coating a colloidal gold suspension on indium tin oxide (ITO) grating structures, which were fabricated by interference lithography and functioned as a waveguide application. The AuNP on the ITO layer were annealed to induce a nanowire formation. This substrate provided strong coupling between the waveguide mode and plasmon resonance of the nanowire [20].

In this study, our objective was the fabrication of a grating-structured substrate for SPR excitation by imprinting solution-processible AuNP onto a grating template. The technique we used provides a simple, rapid and low-cost with high reproducibility. Although the efficacy of the SPR signal is not as favorable as that achieved by using the vacuum evaporation technique, imprinting of AuNP on a grating pattern does provide substrates applicable for SPR measurements. For characterization of the AuNP, their size and size distribution were investigated by localized surface plasmon resonance (LSPR) phenomena [4,5] using UV-visible spectroscopy and a particle analyzer. The morphology of the imprinted AuNP was observed by atomic force microscopy (AFM). Grating-coupled SPR phenomena of the AuNP films were studied using a He-Ne laser as the excitation source and with white light irradiation, which provided multimode excitations of the SP [17-19] on the imprinted AuNP grating substrate. Furthermore, SPR excitation of this substrate was studied by applying a Layer-by-Layer (LbL) deposit of ultrathin films of bis(terpyridine) polymer (Fe(II)-BTP) and poly(3,4-ethylenedioxythiophene):poly(styrenesulfonate) (PEDOT:PSS) [21,22] and observing the spectrum shift of our modified substrate.

EXPERIMENTAL

A chemical reduction method was used to synthesize AuNP, 10.0 mL of 5.07×10^{-4} M hydrogen tetrachloroaurate HAuCl_4 (Wako Pure Chemicals, Japan), was added into 10.0 mL of equivalent molar of sodium borohydride NaBH_4 (Sigma Aldrich, Japan) under vigorous stirring [23-25]. In our synthesis, 2.0 % (w/v) soluble starch (Sigma Aldrich, Japan) was used as a solvent. Moreover, the role of starch molecules was used as a stabilizer in our AuNP synthesis. After HAuCl_4 solution was added into NaBH_4 solution, the color of solution

changed to red color immediately. At final, the AuNP at the concentration of 0.5% (w/v) could be obtained. For fabrication of the imprinted AuNP grating pattern as an SPR excitation substrate, the amount of AuNP must be sufficient to cover the grating substrate and create a uniform grating structure. Thus, AuNP were purified, and the concentration was adjusted to ~20 % (w/v) by centrifugation.

Figure 1a shows the setup for the experimental procedure of AuNP synthesis. For characterization of the AuNP, their extinction spectra were obtained using a UV-visible spectroscope (V-650, JASCO). The size and size distribution were determined by a particle size analyzer (Zetatrac, Microtrac). The imprinted AuNP grating substrate was prepared by the following procedure. A solution of the purified AuNP was dropped onto a silicon grating substrate with a grating pitch size of 1.675 μm . The AuNP solution was dried on the grating pattern under ambient conditions. After drying, the imprinted AuNP grating substrate was annealed at 300 $^{\circ}\text{C}$ for 1 h under air environment before cooling down to room temperature. The imprinted AuNP grating pattern was transferred from the grating substrate to a glass slide using thiolene (Norland optical adhesive 81, NORLAND PRODUCTS Inc, U.S.A.) as a binding chemical. In this process, the thiolene was dropped onto the AuNP film that was then covered with a glass slide. The AuNP grating pattern could be transferred to the glass slide after the thiolene was cured by irradiation with ultraviolet (UV) light for 2 min. The fabrication method for preparing the imprinted AuNP grating pattern is shown in Figure 1b. The AFM image and topology profile of the imprinted AuNP grating pattern were observed by a scanning probe microscope (SPM 9600, SHIMAZU).

For the SPR measurements, SPR reflectivity curves were obtained using a grating-coupling setup that was developed in-house. The excitation source was a He-Ne laser ($\lambda = 632.8 \text{ nm}$). Angular measurements were performed by scanning the incident angle to obtain the reflectivity curves. A halogen lamp was used as the white light source for excitation of multimode SPR. The p-polarized light passed through a pinhole and irradiated the grating sample. Detection was accomplished by a fiber optic spectrometer (USB 2000, Ocean Optics, Inc.). The SP dispersion branches were calculated to determine the multimode of SP with the imprinted AuNP grating.

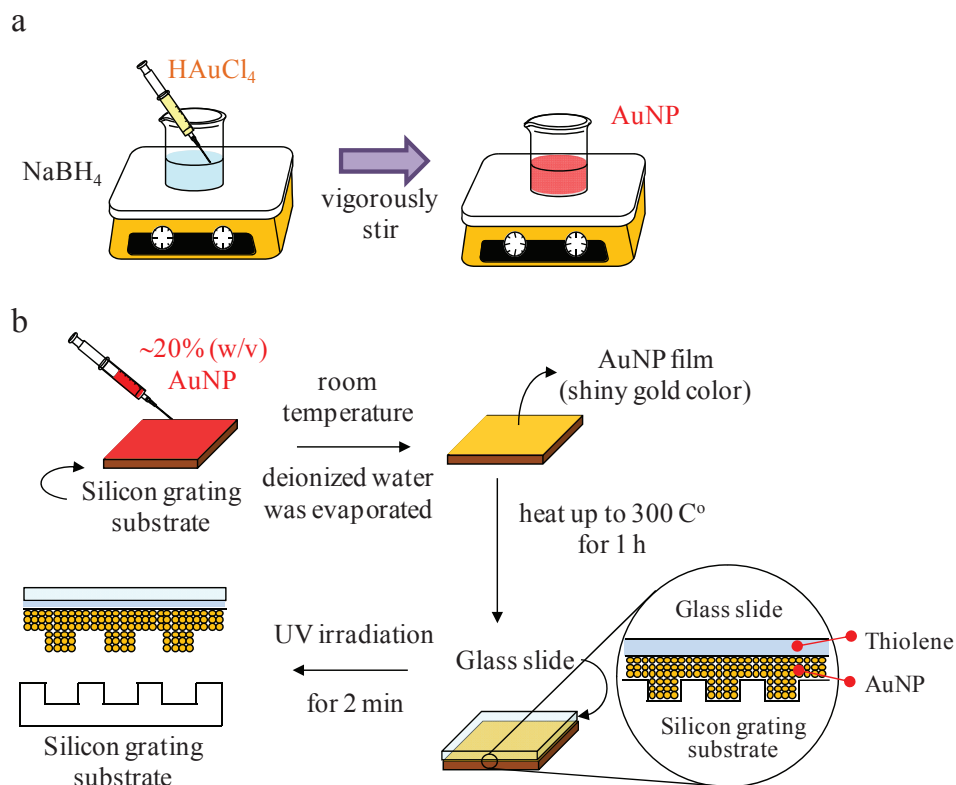


Figure 1 Schematic of the synthesis of AuNP (a) and imprinting of AuNP on a grating pattern (b).

For the grating-coupled SPR excitation, the wave vector of the incident light is increased by the grating vector as the wave vector of the light in air is smaller than that of the SPs [26]. The excitation condition is defined as

$$k_{sp} = k_{px} + G = \frac{2\pi}{\lambda} \sqrt{\varepsilon_m(\omega)} \sin \theta + \frac{2\pi}{\Lambda} m$$

where Λ is the diffraction grating pitch, λ is the wavelength, m is the diffraction order, and $\varepsilon_m(\omega)$ is the wavelength-dependent dielectric constant of gold given by the classical Drude free-electron model.

An ultrathin film of a bilayer system was used to further study SPR phenomena on the imprinted AuNP grating substrate. In this study, the LbL system of Fe(II)-BTP [27] and PEDOT:PSS (Sigma Aldrich, Japan) was employed to investigate the SPR spectral shift. The imprinted AuNP grating substrate was negatively charged with 3-mercaptopropylsulfonic acid sodium salt (MPS) by immersing the substrate into a 1.0 mM of MPS in ethanol for 3 h. The substrate was then rinsed with deionized water for 2 min. The LbL deposition was carried out by immersion of the substrate into a solution of Fe(II)-BTP (0.05 mg/mL) for

15 min. The modified substrate was rinsed with a solution of methanol and water (3:1) for 2 min and then deionized water for 2 min. Subsequently, the substrate was immersed in PEDOT:PSS (10 wt% in deionized water) for 15 min and then rinsed with deionized water for 2 min followed by the 3:1 methanol and water solution for 2 min. The LbL deposition was repeated to form up to 8 bilayers on the substrate surface. The substrate was dried using an air-blower before acquiring the SPR measurements.

RESULTS AND DISCUSSION

Figure 2a shows the normalized UV-visible spectrum of the AuNP (at 10 ppm). As shown in this spectrum, LSPR excitation of the AuNP was observed at 525 nm. The peak position in this region corresponds to the AuNP [28,29]. Figure 2b shows the size and size distribution histogram of the AuNP by using a particles size analyzer. As shown in this figure, the AuNP are in the size range of 20–40 nm with only a few percent of larger particles.

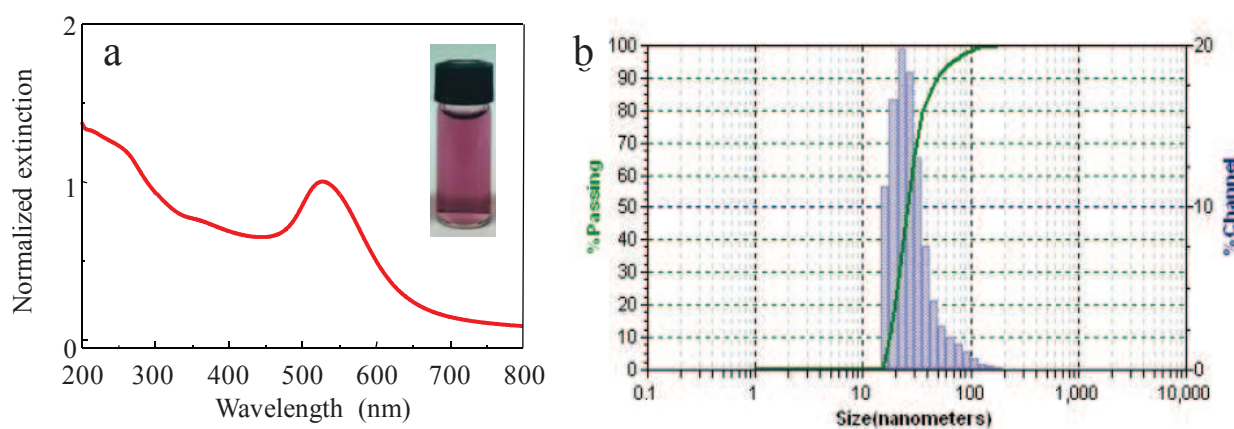


Figure 2 LSPR excitation of AuNP (a) and histogram of the size and size distribution of AuNP (b).

For fabrication of the AuNP film and imprinted AuNP grating pattern as an SPR excitation substrate, the 20% (w/v) AuNP colloid was dropped onto the glass slide and maintained at ambient conditions. The obtained AuNP film is thick enough for the reflection-based grating coupled SPR excitations. After the solvent (deionized water) was evaporated, the shiny gold color of AuNP film could be observed. The morphology of the film was

evaluated by AFM. The AFM images of the AuNP film are shown in Figure 3. As seen in this figure, a high density of AuNP in close contact with nearby particles was achieved. In addition, a densely packed AuNP film can be obtained using the annealing technique, which decreases the grain between the AuNP. This enables the excitation of propagating SPR along the surface of the AuNP film. After the AuNP film was obtained, it was heated up to 300 °C for 1 h. Figure 3b shows AFM images of the AuNP film after annealing. As shown in this figure, the sizes of the AuNP became larger, as if the grain boundary between them had decreased. This result implies that the annealing process induces a sintering phenomenon of AuNP [30,31]. Moreover, the starch molecules, which were added as a stabilizer, should decompose at this temperature [32].

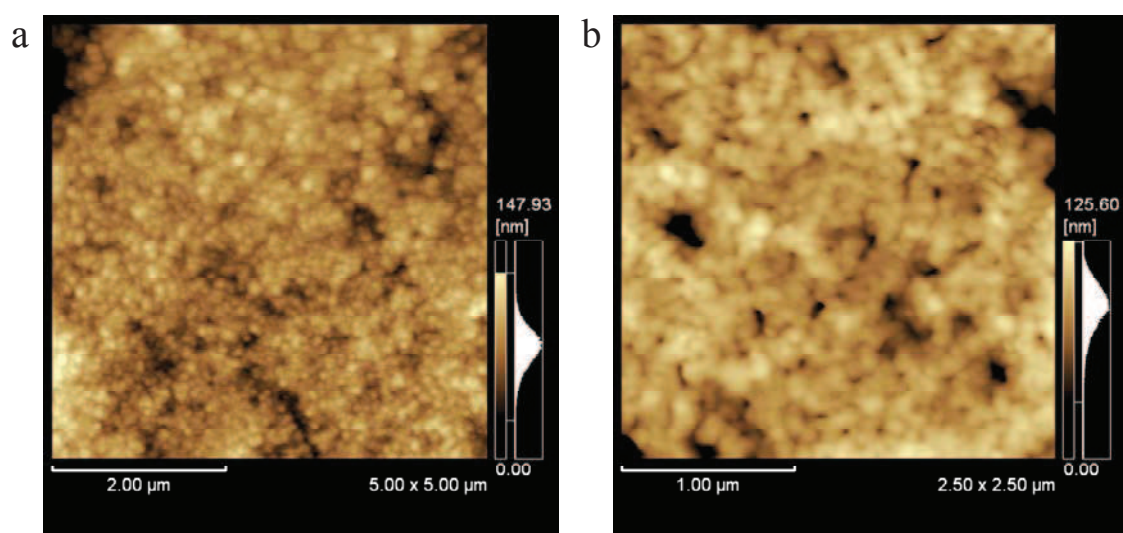


Figure 3 AFM images of AuNP films before (a) and after (b) annealing.

Next, we fabricated an AuNP film on a silicon grating template. A concentrated AuNP colloid was dropped onto the silicon grating. The film was dried and heated up to 300 °C for 1 h under air environment. As schematically shown in Figure 1b, the imprinted AuNP grating pattern was transferred to a glass slide and employed as the SPR grating-coupling substrate. Figure 4 shows the AFM image and topology profile of the imprinted AuNP grating pattern on a glass substrate. The AFM image shows that the grating pitch is 1.72 μm.

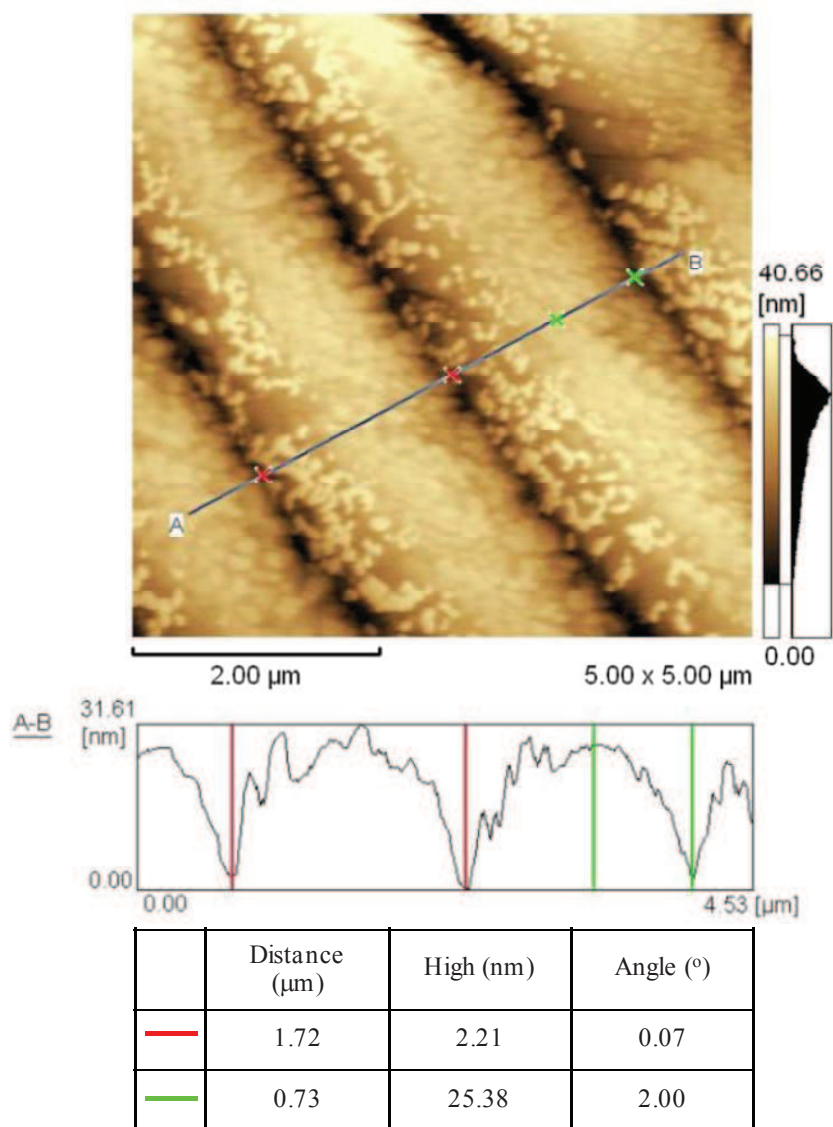


Figure 4 AFM image (a) and topology profile (b) of annealed imprinted AuNP grating pattern.

Then we investigated the SPR phenomena using the fabricated AuNP grating substrate. Figure 5a shows an angular SPR curve of the imprinted AuNP grating film measured at a fixed wavelength of 632.8 nm. For comparison, the SPR curve of a vacuum-evaporated gold grating film is also shown in Figure 5b as a standard SPR property. It should be noted that the grating pitch for the evaporated gold film (1.6 μm) is slightly different from that for the imprinted AuNP. As shown in this figure, a dip due to the SPR excitation was indeed observed. Furthermore, the dip angle (47.1°) is comparable to that of the evaporated Au grating film (43.0°), indicating that the imprinted AuNP can generate the propagating SPR.

Although the peak shape of the imprinted AuNP grating film showed a rather broad and shallow spectrum, the SPR dip angle could be observed distinctively. Figure 6a shows the SPR reflectivity curve of the imprinted AuNP film upon irradiation by white light at a fixed incident angle from 35° to 70° as a function of the wavelength. As shown in this figure, two SPR dips at each wavelength were observed in the regions of 640–700 nm and 760–840 nm. These dips were shown red shift as the incident angle increase. From each SP resonance dip wavelength, the SP dispersion is plotted, as shown in Figure 6b. The calculated SP dispersion relations on the grating corresponding to $m = +5$ ($-SP^{+5}$) and $m = +4$ ($-SP^{+4}$) modes are also shown as solid curves. From the calculated SP dispersion branch, we found that the redshift of SP dips in the range of 640–700 nm and 760–840 nm corresponded well with the $-SP^{+5}$ and $-SP^{+4}$ modes in the SP dispersion, respectively, indicating that our developed substrate indeed provided SPR phenomena. However, due to the incompletely uniform surface of imprinted AuNP, the plotted experimental SP did not completely superimpose on SP dispersion curve as compared to that of evaporated Au grating substrate.

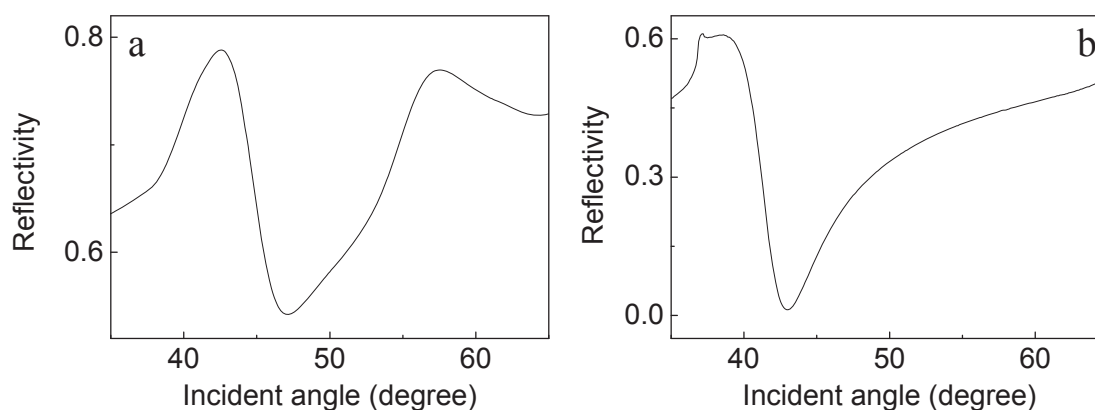


Figure 5 Surface plasmon reflectivity curves of imprinted AuNP grating substrate (a) and evaporated gold grating substrate (b).

To further study the SPR excitation phenomena on the AuNP films, the grating-coupled SPR properties of LbL ultrathin films of Fe(II)-BTP and PEDOT:PSS were studied. As the ultrathin film was deposited on the gold grating surface, the SPR dip angle was shifted to the higher angle. Figure 7 shows the SPR reflectivity curves of an imprinted AuNP grating substrate and an imprinted AuNP/LbL ultrathin film as a function of the incident angle (a) and wavelength (b). Figure 7a shows the SPR dip angle of the imprinted AuNP grating

substrate. The SPR dip angle shifted toward a larger angle (from 47.1° to 50.4°) following LbL film deposition. This result clearly shows that the imprinted AuNP works well as grating-coupled SPR substrates.

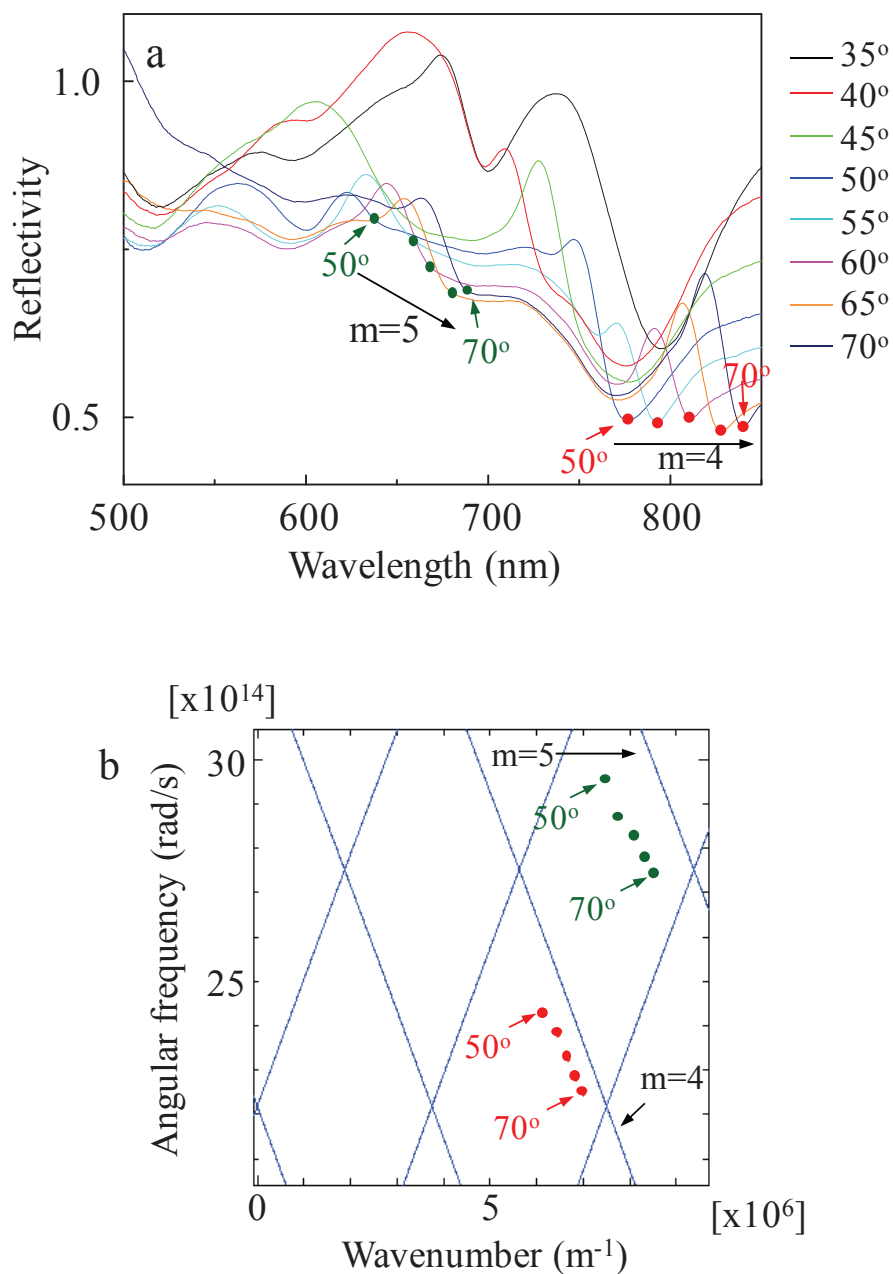


Figure 6 SPR reflectivity curves of imprinted AuNP at a fixed incident angle from 35° to 70° as a function of wavelength (a) and plotted dots obtained from experimental dip angles and calculated SP dispersion (b).

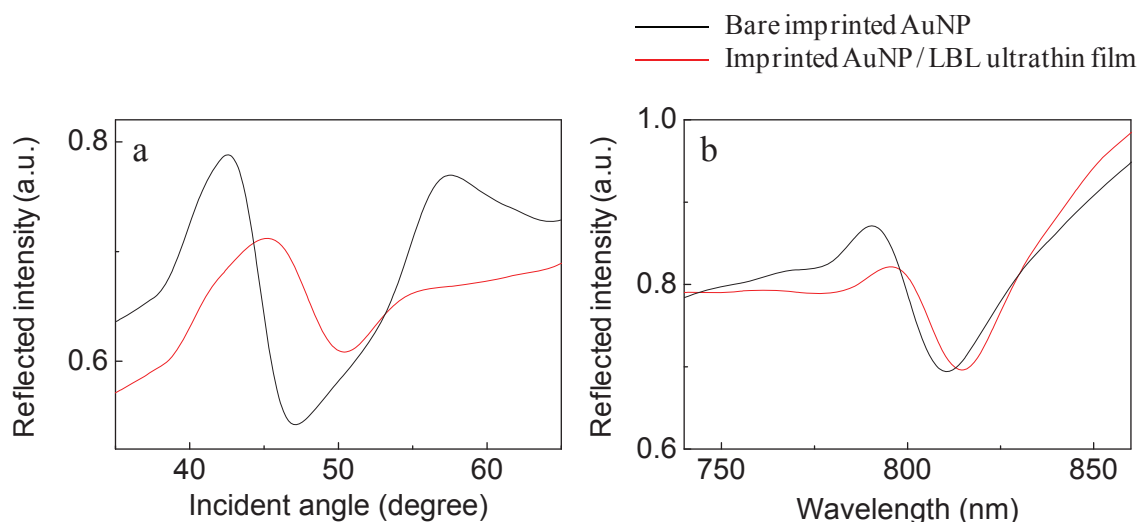


Figure 7 SPR angular curves of imprinted AuNP substrate before and after the deposition of LbL ultrathin film obtained using a He-Ne laser (a) and white light excitation (b).

Figure 7b shows an SPR reflectivity curve of the AuNP grating film upon irradiation with white light as a function of wavelength at a fixed incident angle of 60° . In this case, the SPR dip of the $-SP^{+4}$ mode was observed and spectrum shifted from 810 nm to 815 nm following LbL ultrathin film deposition. These trends correspond well with the SPR properties of standard evaporated gold films (see Figure S4 in supporting information). The results from both SPR techniques imply that the imprinted AuNP grating film is sensitively shifted following deposition of the ultrathin film. Moreover, the imprinted AuNP substrate showed promising data in a dopamine sensor application as the SPR dip showed a red shift with the detection of dopamine (see Figure S5 in supporting information). Hence, the imprinted AuNP grating film could be used as an SPR substrate for a variety of potential applications using grating-coupled SPR devices, such as photoelectric conversions and sensors [17,33-35].

CONCLUSIONS

We successfully developed a method for imprinting AuNP on a grating pattern. The imprinted AuNP grating substrate provided strong surface plasmon resonance excitation signals from both grating-coupling surface plasmon measurements and multimode surface plasmon resonance measurements. This substrate was sensitively shifted when an organic thin film was deposited on the imprinted AuNP grating surface. The imprinted AuNP grating substrate should be useful in photoelectric conversion and sensor applications.

REFERENCES

- (1) H. Wu, L. Wang, J. Zhange, Z. Shen, J. Zhao, Catalytic oxidation of benzene, toluene and *p*-xylene over colloidal gold supported on zinc oxide catalyst, *Catal. Commun.* 12 (2011) 859-865.
- (2) P. Pienpinijitham, X.X. Han, S. Ekgasit, and Y. Ozaki, Highly Sensitive and Selective Determination of Iodide and Thiocyanate Concentrations Using Surface-Enhanced Raman Scattering of Starch-Reduced Gold Nanoparticles, *Anal. Chem.* 83 (2011) 3655–3662.
- (3) N. Cioffi, L. Colaianni, E. Ieva, R. Pilolli, N. Ditaranto, M.D. Angione, S. Cotrone, K. Buchholt, A.L. Spetz, L. Sabbatini, and L. Torsi, Electrocyntesis and characterization of gold nanoparticles for electronic capacitance sensing of pollutants, *Electrochim Acta* 56 (2011) 3713-3720.
- (4) J. Zhao, X. Zhnage, C.R. Yonzon, A.J. Haes, R.P. Van Duyne, Localized surface plasmon resonance biosensors, *Nanomedicine* 1 (2006) 219-228.
- (5) K. A. Willets, R.P. Van Duyne, Localized surface plasmon resonance spectroscopy and sensing, *Annu. Rev. Phys. Chem.* 58 (2007) 267-297.
- (6) J. Deka, A. Paul, A. Chattopadhyay, Sensitive Protein Assay with Distinction of Conformations Based on Visible Absorption Changes of Citrate-Stabilized Gold Nanoparticles, *J. Phys. Chem. C.* 113 (2009) 6936-6947.
- (7) G. Liu, J. Liu, T.P. Davis, J.J. Gooding, Electrochemical impedance immunosensor based on gold nanoparticles and aryl diazonium salt functionalized gold electrodes for the detection of antibody, *Biosens. Bioelectron.* 26 (2011) 3660-3665.
- (8) A. Jyoti, P. Pandey, S.P. Singh, S.K. Jain, R. Shanker, Colorimetric Detection of Nucleic Acid Signature of Shiga Toxin Producing *Escherichia coli* Using Gold Nanoparticles, *J. Nanosci. Nanotechnol.* 10 (2010) 4154-4158.
- (9) L. Zhange, L. Chen, H. Liu, Y. Hou, A. Hirata, T. Fujita, M. Chen, Effect of Residual Silver on Surface-Enhanced Raman Scattering Dealloyed Nanoporous Gold, *J. Phys. Chem. C* 115 (2011) 19583-19587.
- (10) M. Baia, F. Toderas, L. Baia, D. Maniu, S. Astilean, Multilayer Structure of Self-Assembled Gold Nanoparticles SERS and SEIRA Substrate, *ChemPhysChem* 10 (2009) 1106-1111.

- (11) N. Wisitruangsakul, I. Zebger, K.H. Ly, D.H. Murgida., S. Ekgasit, P. Hildebrandt, Redox-linked protein dynamic of cytochrome c probe by time-resolved surface enhanced infrared absorption spectroscopy, *Phys. Chem. Chem. Phys.* 10 (2008) 5276-5286.
- (12) L. Shange, J. Yin, J. Li, L. Jin, S. Dong, Gold nanoparticle-based near-infrared fluorescent detection of biological thiols in human plasma, *Biosens. Bioelectron.* 25 (2009) 269-274.
- (13) W. Knoll, Interfaces and thin films as seen by bound electromagnetic wave, *Annu. Rev. Phys. Chem.* 49 (1998) 569-638.
- (14) J. Homola, I. Koudela, S.S. Yee, Surface plasmon resonance sensors based on diffraction grating and prism couplers: sensitivity comparison, *Sens. Actuators B* 54 (1999) 16-24.
- (15) B. K. Singh, A.C. Hillier, Surface plasmon resonance imaging of biomolecular interactions on a grating-based sensor array, *Anal. Chem.* 78 (2006) 2009-2018.
- (16) B. K. Singh and A.C. Hillier, Surface plasmon resonance enhanced transmission of light through gold-coated diffraction gratings, *Anal. Chem.* 80 (2008) 3803-3810.
- (17) A. Baba, K. Kanda, T. Ohno, Y. Ohdaira, K. Shinbo, K. Kato, F. Kaneko, Multimode surface plasmon excitations on organic thin film/metallic diffraction grating, *Jpn J. Appl. Phys.* 49 (2010) 01AE02-1-01AE02-4.
- (18) A. Baba, N. Aoki, K. Shinbo, K. Kato, F. Kaneko, Grating-coupled surface plasmon enhanced short-circuit current in organic thin-film photovoltaic cells, *ACS Appl. Mater. Interfaces* 3 (2011) 2080-2084.
- (19) A. Baba, K. Wakatsuki, K. Shinbo, K. Kato, F. Kaneko, Increased short-circuit current in grating-coupled surface plasmon resonance field-enhanced dye-sensitized solar cells, *J. Mater. Chem.* 21 (2011) 16436-16441.
- (20) X. Zhang, B. Sun, R.H. Friend, H. Guo, D. Nau, H. Giessen, Metallic Photonic Crystals Based on Solution-Processible Gold Nanoparticles, *Nano Lett.* 6 (2006) 6510-655.
- (21) A. Baba, T. Matsuzawa, S. Sriwichai, Y. Ohdaira, K. Shinbo, K. Kato, S. Phanichphant, F. Kaneko, Enhanced Photocurrent Generation in Nanostructured Chromophore/Carbon Nanotube Hybrid Layer-by-Layer Multilayers, *J. Phys. Chem. C.* 114 (2010) 14716-14721.

- (22) A. Baba, Y. Kanetsuna, S. Sriwichai, Y. Ohdaira, K. Shinbo, K. Kato, S. Phanichphant, F. Kaneko, Nanostructured carbon nanotubes/copper phthalocyanine hybrid multilayers prepared using layer-by-layer self-assembly approach, *Thin Solid Films* 518 (2010) 2200-2205.
- (23) S. Panigrahi, S. Kundu, S.K. Ghosh, S. Nath, T. Pal, General method of synthesis for metal nanoparticles, *J. Nanoparticle Res.* 6 (2004) 411-414.
- (24) M. Luty-Błoch, K. Fitzner, V. Hessel, P. Löb, M. Maskos, D. Metzke, K. Paclawski, M. Wojnicki, Synthesis of gold nanoparticles in an interdigital micromixer using ascorbic acid and sodium borohydride as reducers, *Chem. Eng. J.* 171 (2011) 279-290.
- (25) K.B. Male, J. Li, C.C. Bun, S.C. Ng, J.H.T. Luong, Synthesis and Stability of Fluorescent Gold Nanoparticles by Sodium Borohydride in the Presence of Mono-6-deoxy-6-pyridinium- β -cyclodextrin Chloride, *J. Phys. Chem. C* 112 (2008) 443–451.
- (26) H. Raether, *Surface Plasmons on Smooth and Rough Surfaces and on Grating*, Springer-Verlag, Berlin, 1988.
- (27) F.S. Han, M. Higuchi, D.G. Kurth, Metallosupramolecular Polyelectrolytes Self-Assembled from Various Pyridine Ring-Substituted Bisterpyridines and Metal Ions: Photophysical, Electrochemical, and Electrochromic Properties, *J. Am. Chem. Soc.* 130 (2008) 2073–2081.
- (28) S. Link, M.A. El-Sayed, Size and Temperature Dependence of the Plasmon Absorption of Colloidal Gold Nanoparticles, *J. Phys. Chem. B* 103 (1999) 4212-4217.
- (29) P.K. Jain, K.S. Lee, I.H. El-Sayed, M.A. El-Sayed, Calculated Absorption and Scattering Properties of Gold Nanoparticles of Different Size, Shape, and Composition: Application in Biological Imaging and Biomedicine, *J. Phys. Chem. B* 110 (2006) 7238-7248.
- (30) P.A. Buffat, Lowering of the melting temperature of small gold crystals between 150 Å and 25 Å diameter, *Thin Solid Films* 2 (1976) 283-286.
- (31) K. Nakaso, M. Shimada, K. Okuyama, K. Depper, Evaluation of the change in the morphology of gold nanoparticles during sintering, *J. Aerosol Sci.* 33 (2002) 1061-1074.
- (32) X. Liu, L. Yu, H. Liu, L. Chen, L. Li, In situ thermal decomposition of starch with constant moisture in a sealed system, *Polym. Degrad. Stab.* 93 (2008) 260-262.

- (33) S. Sriwichai, A. Baba, S. Deng, C. Huang, S. Phanichphant, R.C. Advincula, Nanostructured Ultrathin Films of Alternating Sexithiophenes and Electropolymerizable Polycarbazole Precursor Layers Investigated by Electrochemical-Surface Plasmon Resonance (EC-SPR) Spectroscopy, *Langmuir* 24 (2008) 9017-9023.
- (34) A. Baba, P. Taraneekar, R.R. Ponnampati, W. Knoll, R.C. Advincula, Electrochemical Surface Plasmon Resonance and Waveguide Enhanced Glucose Biosensing with *N*-Alkylaminated Polypyrrole/Glucose Oxidase Multilayers, *ACS Appl. Mater. Interfaces* 2 (2010) 2347-2354.
- (35) A. Baba, T. Mannen, Y. Ohdaira, K. Shinbo, K. Kato, F. Kaneko, N. Fukuda, H. Ushijima, Detection of adrenaline on poly(3-aminobenzylamine) ultrathin film by electrochemical-surface plasmon resonance spectroscopy, *Langmuir* 26 (2010) 18476-18482.

CHAPTER III

Transmission Surface Plasmon Resonance Signal Enhancement via Growth of Gold Nanoparticles on a Gold Grating Surface

Chutiparn Lertvachirapaiboon^{1,2}, Chirayut Supunyabut², Akira Baba^{1*}, Sanong Ekgasit^{2*}, Chuchaat Thammacharoen², Kazunari Shinbo¹, Keizo Kato¹,
and Futao Kaneko¹

¹ Graduate School of Science and Technology and Center for Transdisciplinary Research, Niigata University, 8050 Ikarashi 2-nocho, Nishi-ku, Niigata 950-2181, JAPAN.

² Sensor Research Unit, Department of Chemistry, Faculty of Science, Chulalongkorn University, 254 Phayathai Rd., Patumwan, Bangkok 10330, THAILAND.

This article has been published in Journal: Plasmonics.

Volume: 8, Pages: 369-375, Year: 2013.

ABSTRACT

We developed a novel technique for increasing the sensitivity of transmission surface plasmon resonance (T-SPR) signals. T-SPR spectroscopy was performed by irradiating, with white light, a gold grating substrate whose surface was nanostructured by growing gold nanoparticles (AuNPs). AuNPs were grown directly on the substrate surface by alcohol reduction and their growth was observed at various stages by UV-visible spectroscopy and standard Kretschmann-type SPR spectroscopy. For comparison, normal gold film with smooth surface was examined under the similar condition. The T-SPR results show a possibility of hybrid excitation of both localized and propagating surface plasmon. Significantly, T-SPR spectra of the gold grating substrate obtained during AuNPs growth show stronger and narrower peaks in the range 650–800 nm. The maximum T-SPR excitation was at an incident angle of 35°. A layer-by-layer system of 5, 10, 15, 20-tetrakis (1-methyl-4-pyridinio) porphyrin tetra (*p*-toluenesulfonate) molecules and sodium copper chlorophyllin molecules was used to verify the enhancement of the developed system. We believe that the AuNPs/Au grating for T-SPR devices will provide enhanced signals for detecting nanometer order materials and for high-sensitive sensor applications.

INTRODUCTION

Surface plasmon resonance (SPR) on a diffraction grating is widely used to characterize and study ultrathin films, analytical surface binding, biomolecules immobilization, and surface kinetic processes [1, 2]. Various types of grating structures can be used for SPR excitation. The flexibility and simplicity of the system make grating-based SPR a research topic of significant interest [1-10]. SPR excitation has recently been shown to enhance light transmission through nanostructures such as hole arrays [11, 12] and grating patterns [8-10] and, of particular interest, through grating substrates of commercial digital versatile disc-recordables (DVD-Rs) coated with thin gold films [6, 7]. Significantly, transmission SPR (T-SPR) spectra of light transmitted through such a gold grating substrate show strong, narrow peaks in the visible light region. The T-SPR wavelength depends on the grating pitch and the angle of incidence [6, 7]. Recently, diffraction-based surface enhanced transmission was reported that the ± 1 diffracted orders from the gold grating film were detected [13]. The optical transmission is based on the decoupling of surface plasmons which is excited and confined at the surface of metals. Hence, the T-SPR spectrum is highly sensitive to the local refractive index near a metal/dielectric interface, making T-SPR spectroscopy a useful

technique for optical sensing applications. The sensitivity depends especially on the surface structures for the coupling of near field SP excitations and decoupling to far field freely propagating light [14-16]. However, to our knowledge, there is no report to further enhance the T-SPR signals with the modification of the nanostructured surfaces.

In this study, we investigate whether a T-SPR signal, known to be enhanced by transmission through a gold grating substrate, can be enhanced even further if the surface structure of the gold grating is modified with gold nanoparticles (AuNPs). The benefit of AuNPs deposition is that it enhances the excitation of SPR and facilitates decoupling of SPs. Furthermore, it may also excite hybrid SPs by localized SPR (LSPR) and grating-coupled propagating SPR. AuNPs without any capping agent can be directly grown on the gold grating surface by alcohol reduction [17, 18]. Gold particles on the gold grating surface can induce AuNPs nucleation and thus seed AuNPs growth [19]. Furthermore, the T-SPR sensitivity of an deposited organic ultrathin films was enhanced via AuNPs on the gold grating.

EXPERIMENTAL

We investigated AuNPs growth on a gold grating surface and, for comparison, on a smooth gold film surface. A growth solution of hydrogen tetrachloroaurate (HAuCl_4) in ethanol was prepared by mixing HAuCl_4 (0.25 M, 1.0 mL) with ethanol (40% v/v) and adjusting to a volume of 100 mL. For growing AuNPs on a gold grating surface, a polycarbonate DVD-R (Taiyo Yuden Co., Ltd.) was used as the diffraction grating substrate. The DVD-R was cut into pieces, which were then immersed in nitric acid to remove the dye layer on the grating side. The cleaned pieces were coated with a layer of gold (thickness ~50 nm) by vacuum evaporation. The resulting substrate is denoted as bare Au grating substrate. AuNPs were grown directly on the grating surface by immersing the coated substrate in the growth solution. The resulting substrate containing AuNPs grown on the gold-coated grating is denoted as AuNPs/Au grating substrate. Figure 1 shows the experimental procedure of the growth process.

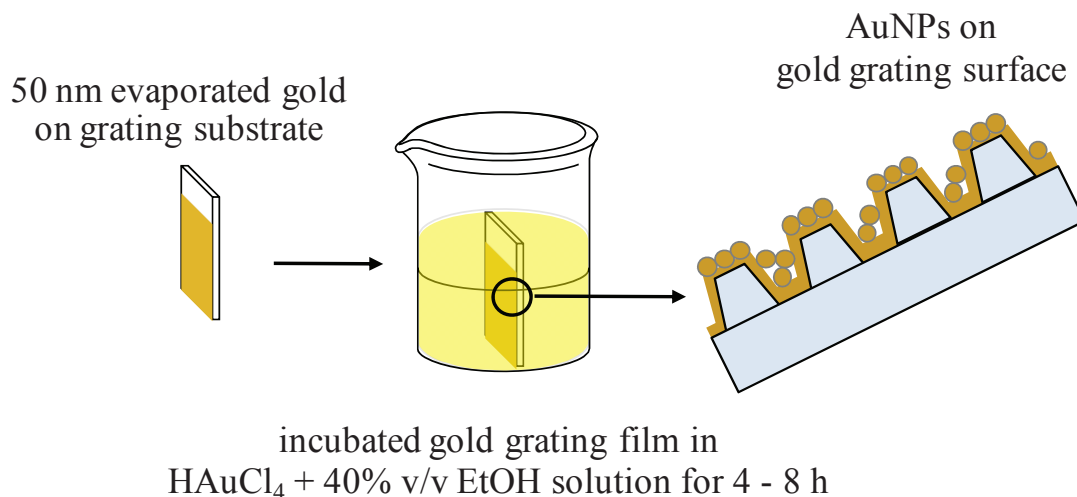


Figure 1 Experimental procedure for growing gold nanoparticles on a gold-coated grating surface.

For AuNPs growth on a flat gold film (thickness ~ 30 nm) surface, gold films on BK7 ($n=1.52$) glass slides were immersed several times in the growth solution. The resulting substrate containing the gold coating is denoted as Au film substrate. AuNPs growth was monitored by UV-visible spectroscopy (V-650 UV-visible spectroscope, JASCO) and prism-coupled SPR spectroscopy by using the Kretschmann configuration [20-22] with the excitation wavelength at 632.8 nm (He-Ne laser). Moreover, the thickness of gold film was calculated by fitting the SPR reflectivity curves with a Fresnel equation algorithm (Winspill software version 2.20). The morphologies of the bare Au grating and the AuNPs/Au grating surfaces were examined by atomic force microscopy (AFM) (SPM-9600, SHIMAZU).

T-SPR measurements were conducted with a homemade T-SPR system equipped with a fiber optic spectrometer (HR 4000, Ocean Optics, Inc.) and a white light source (LS-1 tungsten halogen, Ocean Optics, Inc.). The substrates were mounted on a rotation stage. White light was passed through a linear polarizer and the T-SPR signal of the gold grating and AuNPs/Au grating substrates were then detected by fiber optic spectrometry. Figure 2 shows the schematic diagram of the instrumental setup. To clearly show the effect of surface plasmon enhanced transmission light spectrum, a normalized spectrum was constructed by subtracting the raw spectrum of s-polarized light from that of p-polarized light.

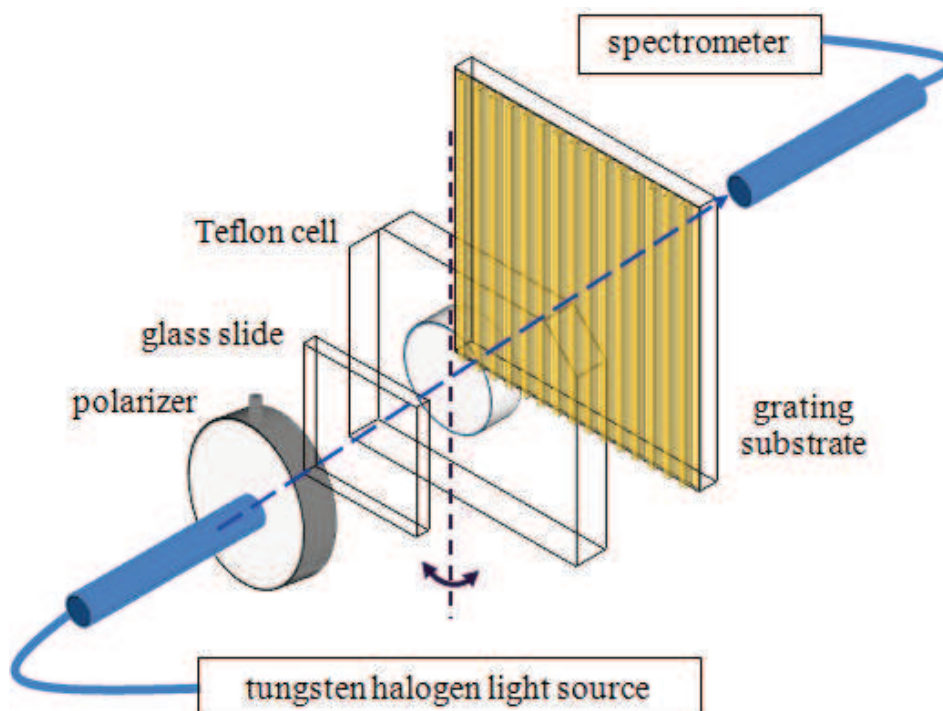


Figure 2 Schematic diagram of the T-SPR instrumental setup.

T-SPR enhancement was verified by investigating the substrates after coating with a multilayered ultrathin film. The bare Au and AuNPs/Au grating surfaces were charged negatively with 3-mercaptopropionic acid sodium salt (MPS) by soaking the substrate in 1.0 mM of MPS for 3 h. The substrate was rinsed by deionized water for two times for 1 min each before the substrate was coated with multilayer film. The multilayered film was then obtained by layer-by-layer electrostatic deposition [23, 24]. In this experiment, the cationic and anionic molecules were 5, 10, 15, 20-tetrakis (1-methyl-4-pyridinio) porphyrin tetra (*p*-toluenesulfonate) (TMPyP) and sodium copper chlorophyllin (SCC), respectively [5, 25, 26]. The sequential adsorption of cationic and anionic molecules was performed by alternate immersion in TMPyP and SCC solution at the concentration of 0.25 mM into for 15 min each. Between the chemical was alternated, they were rinsed by deionized water for two times for 1 min each. The injection cycle was carried out up to 10 bilayers on the substrate surface.

RESULTS AND DISCUSSION

First, we simulated the electric field of Au grating and nanostructured Au grating structures using the FDTD method (FDTD solutions) to study the possibility of enhancement in T-SPR signals. Figure 3 shows the electric fields of water/rectangle Au (thickness 50 nm) grating with and without rectangle Au islands on the polycarbonate grating substrates (grating pitch, $\Lambda = 740$ nm) upon irradiation with p-polarized light at a wavelength of 740 nm at an incident angle of 35° . The assumed nanostructured surfaces, 10 nm width and 5 nm height Au islands and 100 nm width and 10 nm height Au islands, of Au grating thin films (thickness 50 nm), are also shown in the figure 3c and 3d. These structures are similar to the dispersed AuNPs or AuNPs aggregation on Au grating films used in our experiments. The color bar shows the electric field intensity. In the simulation, the refractive index of polycarbonate is 1.585. Palik parameters were used the dielectric constant of Au [27]. As shown in Figure 3b, a strongly enhanced electric field was observed on the water side of Au, indicating the excitation of the surface plasmons. It should be noted that light is transferred through the continuous thin gold grating film (thickness 50 nm) as seen in the near field on the polycarbonate side. As seen in figure 3, the electric field intensity further increases when the Au islands exist on the Au grating. The enhancement is observed in both Au islands structures (Figure 3c and 3d), which might be due to the interaction between the grating coupled-propagating surface plasmon and the nanoscaled Au islands. This result indicates the possibility that the enhancement in the near field surface plasmon excitation can be obtained when the nanostructured surface is fabricated on the thin Au grating film, indicating the possibility of the enhancement of T-SPR signals.

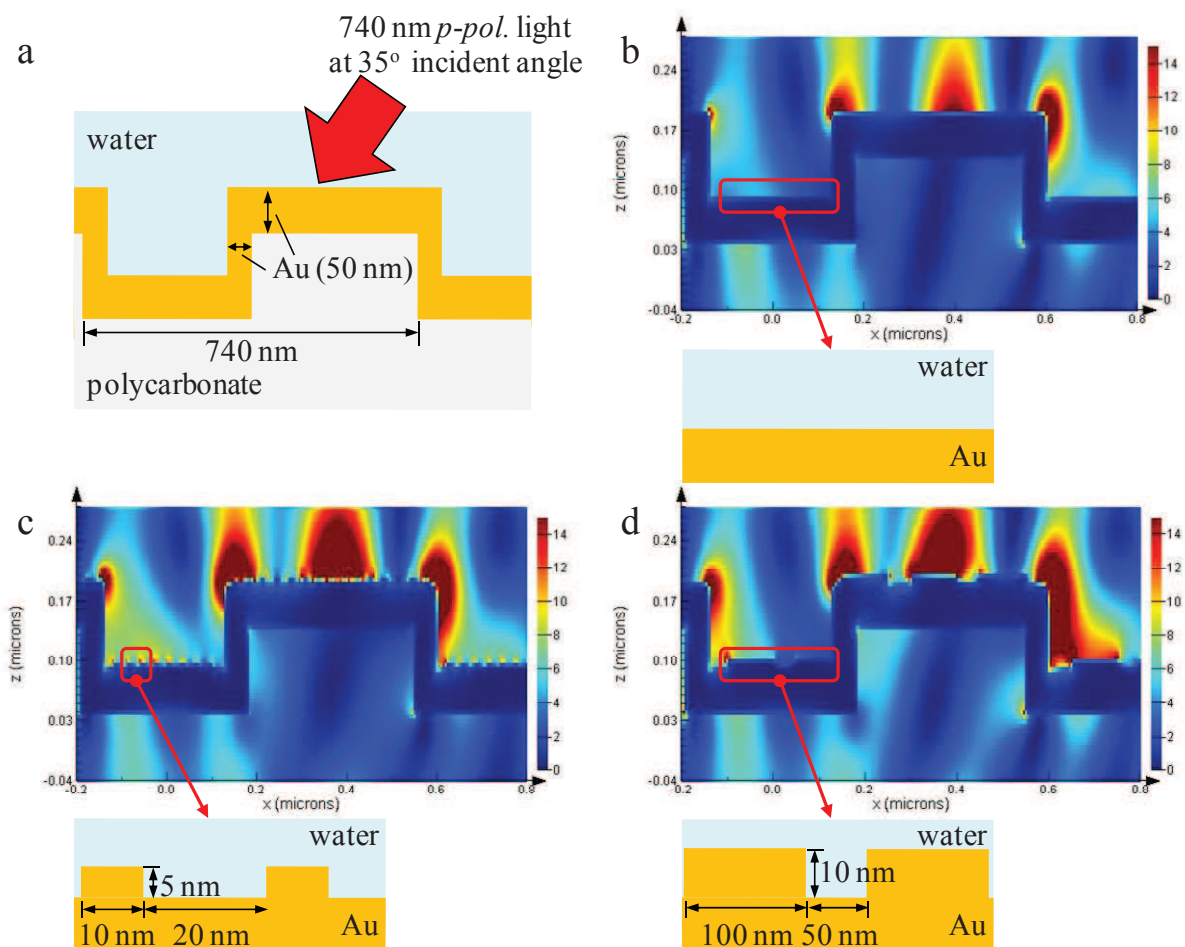


Figure 3 Schematic drawing of Au grating film with gold (thickness 50 nm) polycarbonate grating structure (grating pitch, $\Lambda = 740$ nm) (a). Electric field of Au grating film (b), AuNPs (small particles)/Au grating film (c) and AuNPs (large particles)/Au grating film (d) in the environment of water and the enlargement of schematic drawing which corresponds with AuNPs on the gold grating used in our experiments.

To fabricate the nanostructured Au surface, we tried to grow AuNPs directly on Au thin films. Figure 4 shows UV-visible spectra of AuNPs grown on the flat Au film substrate, obtained at various incubation times. At 2 h of incubation, the spectrum baseline is almost the same as that of the Au film substrate, indicating virtually no AuNPs deposition. At 4 h of incubation, a peak at 525 nm (the enlarged spectrum is shown in the inset), attributing to LSPR excitation from AuNPs [28], was observed on the flat Au thin film. Because propagating SPR can be excited on the flat Au thin film, this result suggests a possibility that we may be able to obtain hybrid LSPR and propagating SPR excitation on the Au film surface, which is useful for enhancing sensitivity in biosensor applications [29, 30]. At 6 h of

incubation, the LSPR excitation intensity increases and redshift from 525 to 545 nm was observed. This result implies that the gold salt is reduced to AuNPs and the existing AuNPs continue to grow. In addition to the redshift of LSPR wavelength, the spectral baseline raises, indicating that AuNPs deposition causes the film thickness to increase. After 8 h of incubation, the baseline raises even further, indicating that AuNPs may continue to grow on the Au film surface.

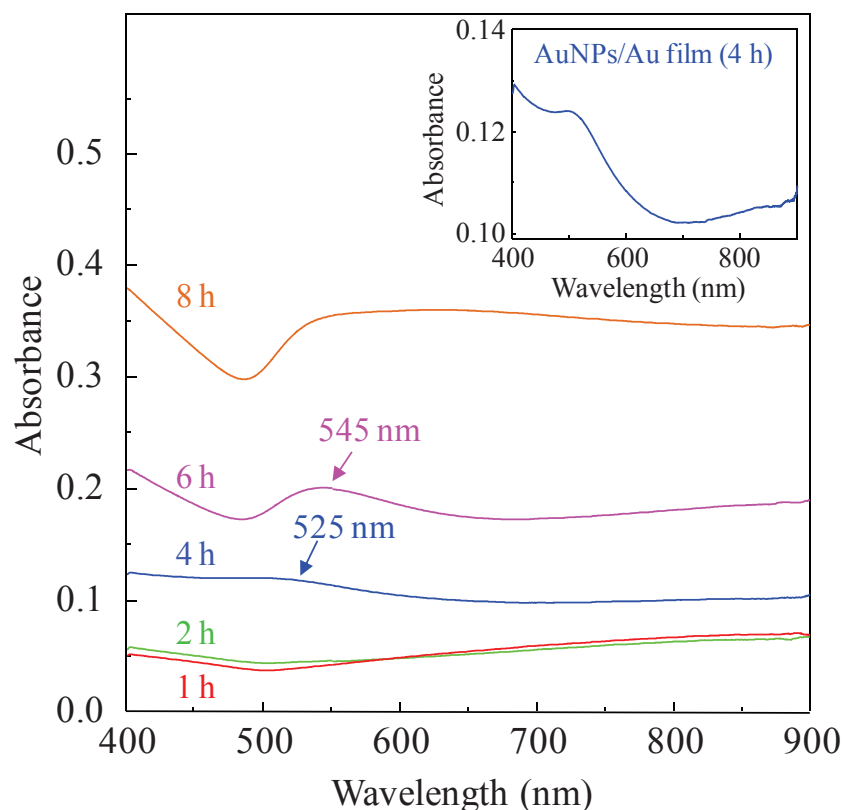


Figure 4 UV-visible spectra of AuNPs grown on Au film substrate, obtained at various incubation times and the inset spectrum shows the enlargement of UV-visible spectrum of AuNPs grown on Au film substrate at 4 h incubation.

Figure 5a shows the SPR spectra of AuNPs grown on the flat Au film substrate, obtained at various incubation times. The curve of the bare Au film is shallow because the film thickness is just 34 nm. As incubation time increases, the dip angle of the curve shifts from 45.0° to 47.3° . Between 1 and 4 h of incubation, the reflection intensity decreases. At 4 h the curve dips sharply to the lowest reflectivity with the SPR angle of 46.2° . After 4 h, the reflectivity increases while the SPR angle shifts to 47.3° . The sharp dip indicates strong

SP excitation from Au/AuNPs. This trend in SPR properties is similar to our previous simulation results which assumed that AuNPs are present on the gold surface [31, 32]. Thus, this result indicates the presence of AuNPs on the gold film surface [19]. Incubation for just a few hours is known to cause both AuNPs diameter [22] and density [31, 32] to increase. Thus, the observed change in the SPR dip angle of the AuNPs on the Au film substrate should be due to the damping effect of AuNPs [20-23]. At 8 h of incubation, the dip becomes shallower. SPR shifts associated with scattering and absorption by surface roughness are well defined [33]. Hence, this result suggests that AuNPs cause the surface to become rougher.

Figure 5b shows the plot of the Au film thickness as a function of incubation time. The slope of the fitting curve can be split into two regions, indicating that gold growth occurs in two phases. In the first phase of growth, the total film thickness increases as the gold surface seeds AuNPs nucleation. It should be noted that the AuNPs used in these experiments contain no capping agents; hence, they should aggregate smoothly on the film surface and form thin film of AuNPs. Simulations suggest that during this first phase, the film thickness increases by ~ 1.6 nm. After 3 h of incubation, the AuNPs growth rate on the evaporated gold surface changes. In the second phase of growth, i.e., with the incubation time beyond 3 h, the UV-visible spectrum shows LSPR excitation from AuNPs indicating an existence of AuNPs on the evaporated gold film. A simulation based on SPR reflectivity results shown in Figure 3 indicated that AuNPs size at 4 h incubation is 9.7 nm.

Figure 6 shows AFM images of the bare Au grating and the AuNPs/Au grating surfaces during incubation. Roughness (R_a) of the bare Au grating surface increases with incubation time. In particular, before incubation, roughness is 1.7 nm. At 4, 6, and 8 h of incubation, roughness increases to 2.6, 3.1, and 6.5 nm, respectively. This result confirms that AuNPs can indeed grow on a gold surface. At 6 and 8 h of incubation, the grating pattern becomes non-uniform as AuNPs appear on the surface.

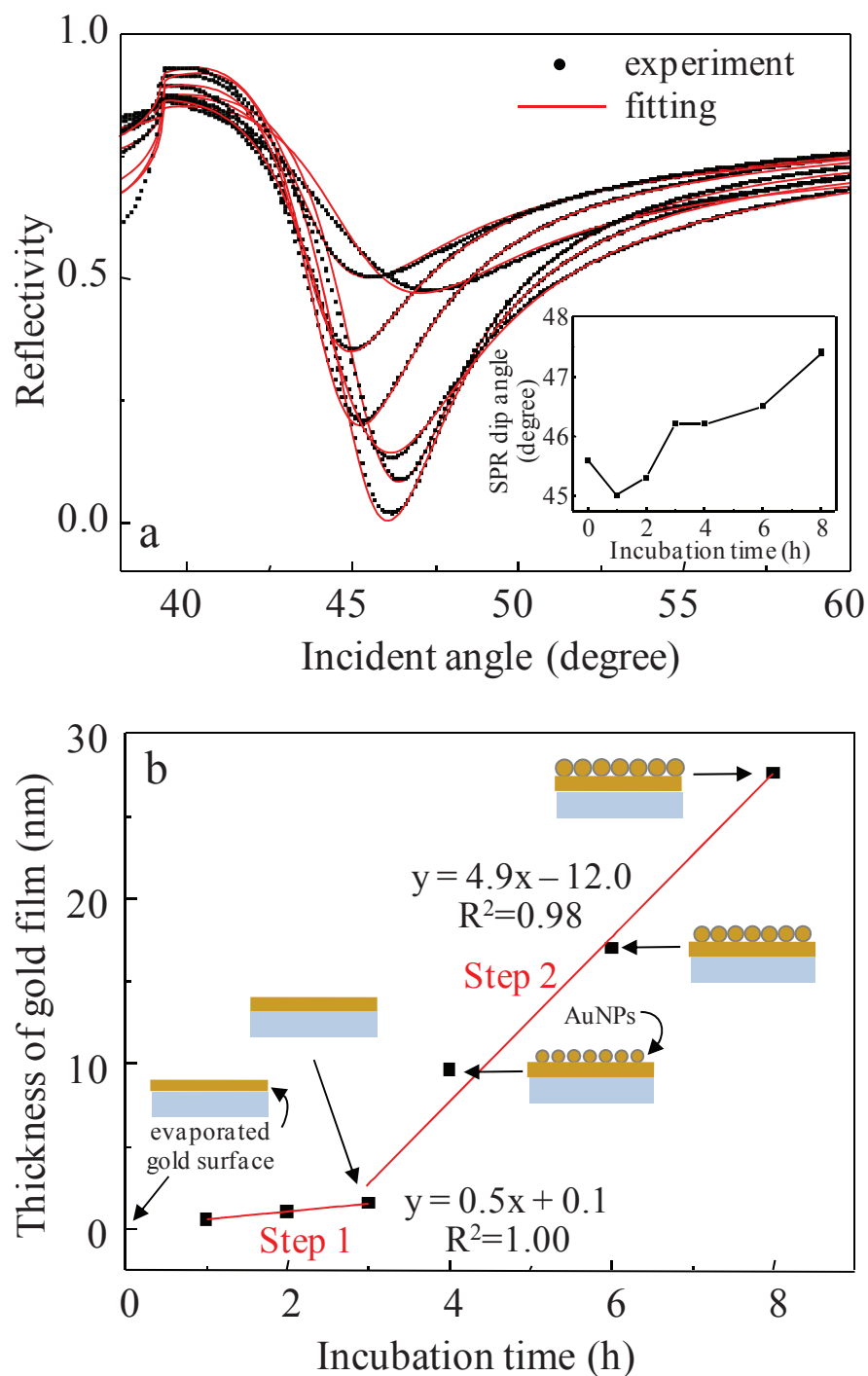


Figure 5 SPR experimental and fitted SPR curves of AuNPs grown on Au film substrate obtained at various incubation times (a) (The inset shows the SPR dip angle as a function of incubation time). Plot of Au film thickness as a function of incubation time (b).

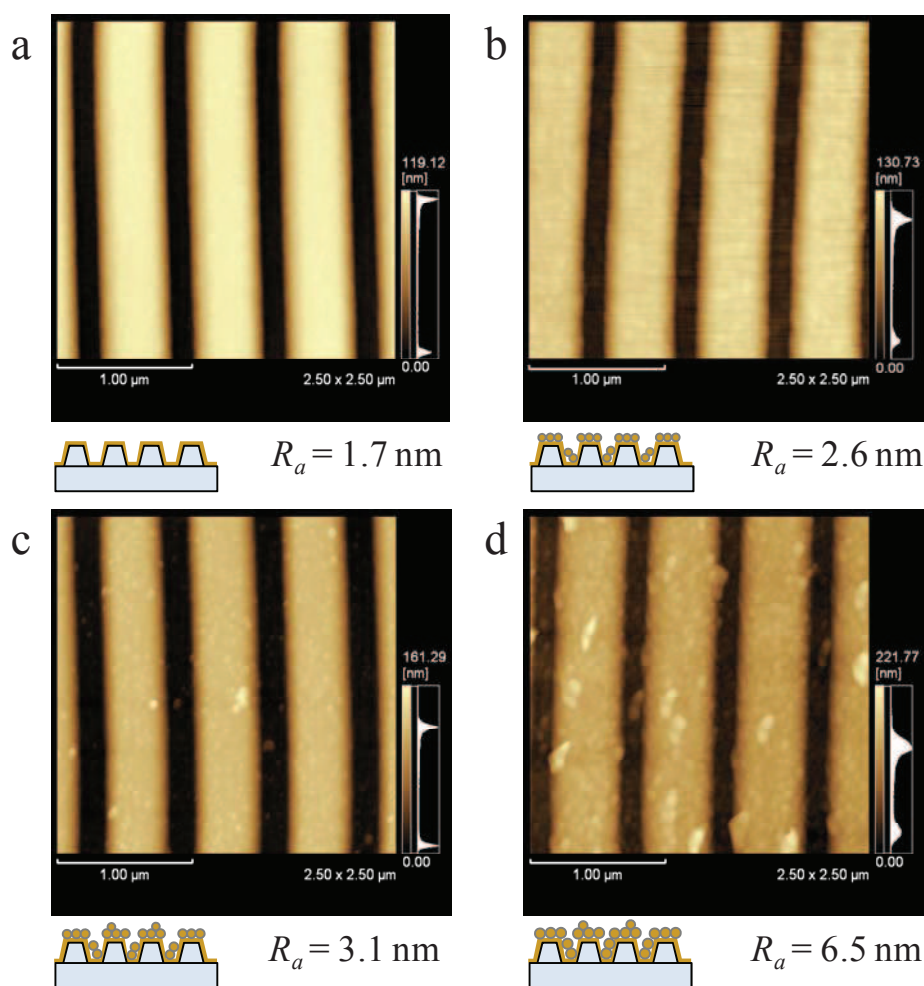


Figure 6 AFM image of bare Au grating surface (a), AuNPs/Au grating surfaces with incubation time of 4 (b), 6 (c), and 8 h (d). The corresponding schematic drawing of gold nanoparticles on the gold grating at the given incubation time is proposed.

Figure 7 shows T-SPR spectra of the bare Au grating and AuNPs/Au grating substrates after incubation for 4 h, measured at incident angles in the range $\theta = 25^\circ\text{--}40^\circ$ in a water environment. For both substrates, peaks are observed in the range 700–800 nm. As the incident angle increases from 25° to 30° , the spectra shift to shorter wavelength; beyond 30° , the spectra shift to longer wavelength, indicating that the T-SPR peak is sensitive to the incident light angle. For both substrates, the maximum T-SPR intensity is observed at 35° . As shown in the Figure, the peak of Au/AuNPs after incubation is indeed sharper than that of Au, possibly because the nanostructured surface of the AuNPs/Au grating substrate excites stronger SPs and facilitates decoupling of the excited SPs on the grating surface. This result corresponds well with FDTD simulation that the near field surface plasmon enhancement

increases the intensity of decoupled T-SPR intensity. It should be noted that the flat Au film on polycarbonate grating was controlled to be ~ 50 nm, hence the sharpened T-SPR peak is not due to the increased film thickness, but due to the present of AuNPs.

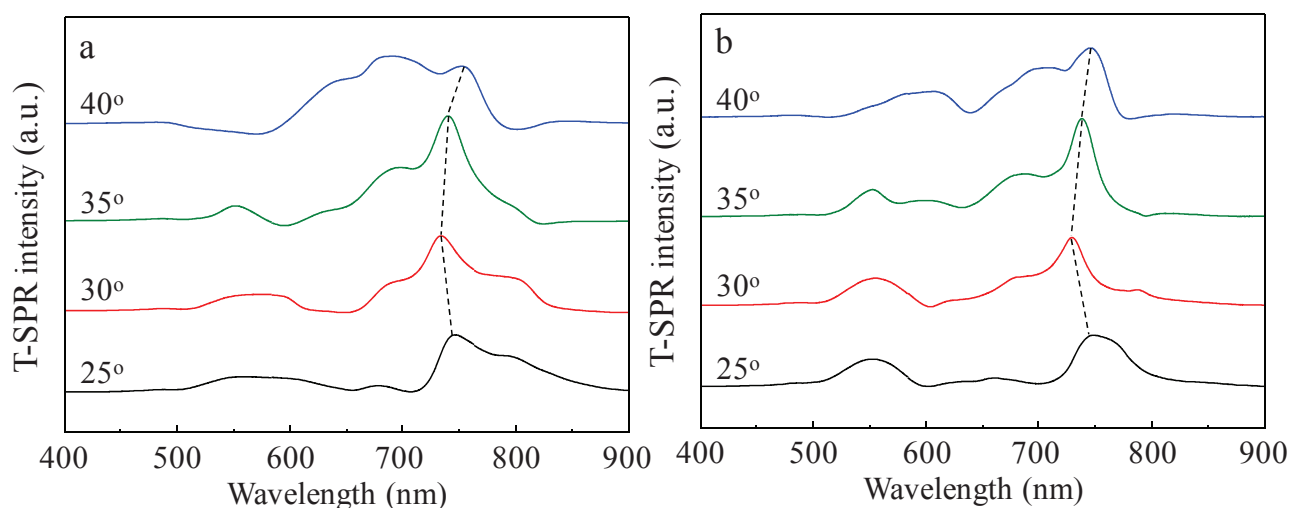


Figure 7 T-SPR spectra with the angle of incidence of 25 – 40° of the bare Au grating substrate (a) and that of AuNPs/Au grating substrate with 4 h incubation (b). The angle of incident is indicated above the corresponding spectrum.

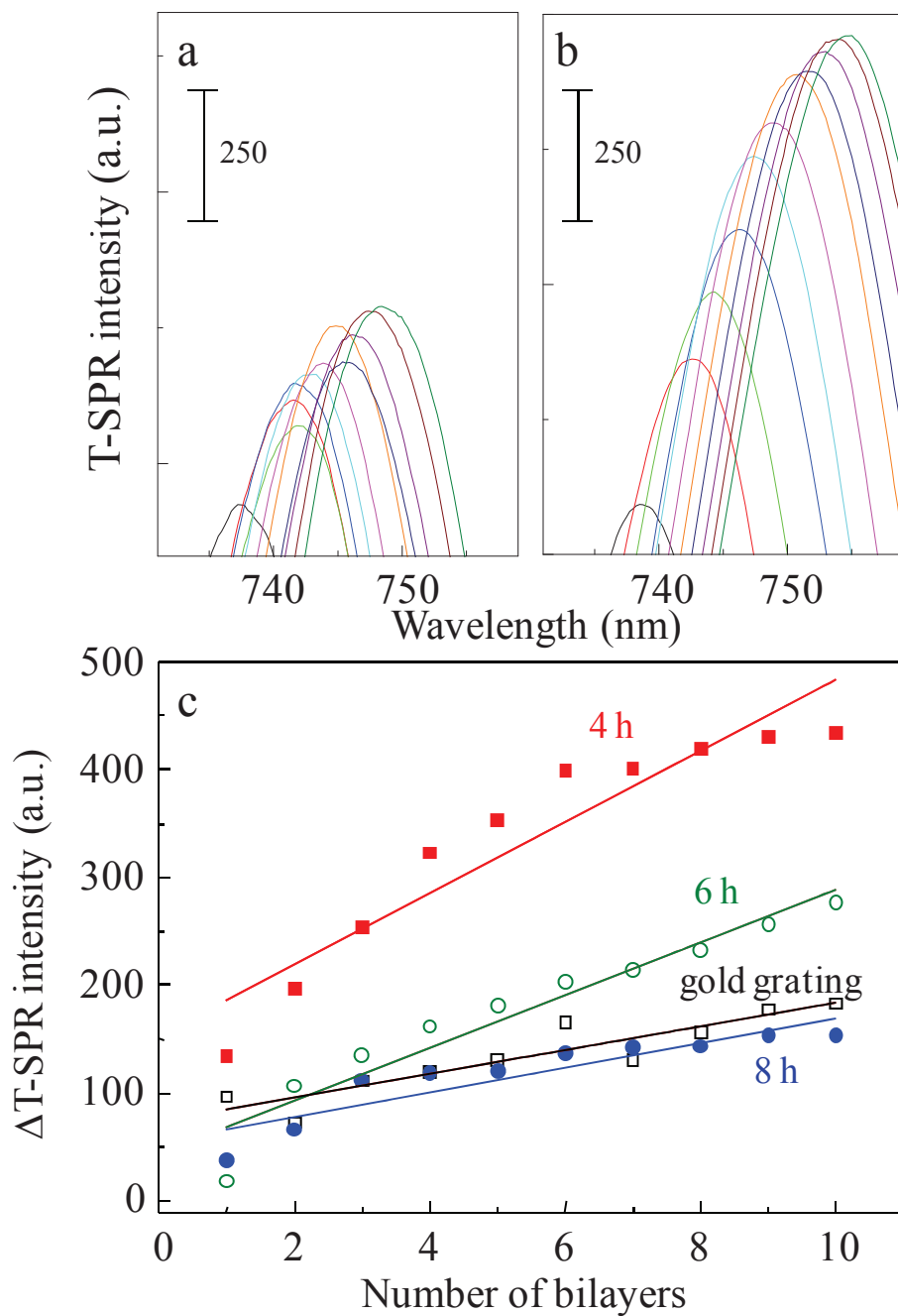


Figure 8 T-SPR spectra of bilayers fabricated on substrate monitored at the angle of incidence 35° : bare Au grating substrate (a), AuNPs/Au grating substrate with 4 h incubation (b), and plots of changes in the T-SPR intensity as a function of the number of bilayers (c) on bare Au grating substrate (open square, black), AuNPs/Au grating substrate with 4 h (filled square, red), 6 h (open circle, green), and 8 h (filled circle, blue) incubations.

Because both bare Au grating and AuNPs/Au grating substrates show strong T-SPR peaks at 35° , we monitored the change in the T-SPR intensity at an incident angle of 35° during the deposition of the layer-by-layer ultrathin film on both types of substrate to examine the T-SPR signal sensitivity with respect to the adsorption of nanometer size materials using our developed surface. We fabricated the multilayered film by alternately functionalizing the substrate with negatively charged MPS for adsorption of cationic TMPyP and immersing the substrate in anionic SCC solution. Figure 8a and b shows the T-SPR spectra of the various bilayers on the bare Au grating and the AuNPs/Au grating substrates after 4 h of incubation. The changes of T-SPR intensity as a function of the number of bilayers is shown in Figure 8c. Although the intensity seems to be saturated when the number of bilayers increase, the intensity is increased with the number of bilayers for all cases. From the simulation, the trend of the T-SPR intensity change largely depends on grating structures, grating pitch, etc. The AuNPs/Au grating substrate shows a large increase in the T-SPR intensity, particularly the substrate with 4 h incubation, which shows spectral redshift while the intensity increases much larger than that of the bare Au grating substrate. This result also corresponds well with the strong SP excitation observed in Figure 5a and FDTD simulation. Thus, we conclude that the nanostructure generated by the AuNPs on the surface of gold grating after 4h enhances the signal sensitivity on the AuNPs/Au surface. When the incubation time exceeds more than 4 h, the shift of T-SPR intensity gradually decreased. In the case of after 8 h, the T-SPR intensity change was slightly smaller than that on the Au grating. The smaller change in the T-SPR peak intensity after 8h should be due to the weak SP excitation originating from roughened Au grating surface with randomly aggregated AuNPs. This finding is reasonable because a high degree of surface roughness decreases excitation of SPs, as observed in Figure 5a.

CONCLUSIONS

We fabricated AuNPs on a Au grating substrate by chemical reduction of a gold salt with ethanol. AuNPs grew on the substrate after incubation for 4 h in the growth solution. Examination of the resulting AuNPs/Au grating substrate by UV-visible and SPR spectroscopy shows the possibility of hybrid LSPR and propagating SPR excitation. The presence of AuNPs on the substrate surface increases the excitation of surface plasmons and facilitates decoupling at the back side of Au grating which corresponds well with the results of FDTD simulation. When a multilayered film is deposited on the treated substrate and the

change in the T-SPR intensity is measured as a function of the number of bilayers, the largest enhancement is observed for the AuNPs/Au grating substrate incubated for 4 h. Thus, we conclude that the nano-rough surface induced by AuNPs film improves T-SPR sensitivity of the Au grating substrate. The present study should be useful for the characterization of nanometer order materials and for biosensor applications.

REFERENCES

1. Knoll W (1998) Interfaces and thin films as seen by bound electromagnetic wave. *Annu. Rev. Phys. Chem.* 49:569-638
2. Homola J, Koudela I, Yee SS (1999) Surface plasmon resonance sensors based on diffraction gratings and prism couplers: sensitivity comparison. *Sens. Actuators B* 54:16-24
3. Baba A, Kanda K, Ohno T, Ohdaira Y, Shinbo K, Kato K, Kaneko F (2010) Multimode surface plasmon excitations on organic thin film/metallic diffraction grating. *Jpn. J. Appl. Phys.* 49:01AE02-1-01AE02-4
4. Baba A, Aoki N, Shinbo K, Kato K, Kaneko F (2011) Grating-coupled surface plasmon enhanced short-circuit current in organic thin-film photovoltaic cells. *ACS Appl. Mater. Interfaces* 3:2080-2084
5. Baba A, Wakatsuki K, Shinbo K, Kato K, Kaneko F (2011) Increased short-circuit current in grating-coupled surface plasmon resonance field-enhanced dye-sensitized solar cells. *J. Mater. Chem.* 21:16436-16441
6. Singh BK, Hillier AC (2006) Surface plasmon resonance imaging of biomolecular interactions on a grating-based sensor array. *Anal. Chem.* 78:2009-2018
7. Singh BK, Hillier AC (2008) Surface plasmon resonance enhanced transmission of light through gold-coated diffraction gratings. *Anal. Chem.* 80:3803-3810
8. Xu ZC, Dong B, Xue J, Yang R, Lu BR, Deng S, Li ZF, Lu W, Chen Y, Huq E, Qu XP, Liu R (2010) Surface plasmon polariton coupling induced transmission of subwavelength metallic grating with waveguide layer. *Microelectron. Eng.* 87:1297-1299
9. Turker B, Guner H, Ayas S, Ekiz OO, Acar H, Guler MO, Dâna A (2010) Grating coupler integrated photodiodes for plasmon resonance based sensing. *Lab Chip* 11:282-287

10. Yeh WH, Kleingartner J, Hillier AC (2010) Wavelength tunable surface plasmon resonance-enhanced optical transmission through a chirped diffraction grating. *Anal. Chem.* 82:4988-4993
11. Ebbesen TW, Lezec HJ, Ghaemi HF, Thio T, Wolff PA (1998) Extraordinary optical transmission through sub-wavelength hole arrays. *Nature* 391:667-669
12. Brolo AG, Gordon R, Leathem B, Kavanagh KL (2004) Surface plasmon sensor based on the enhanced light transmission through array of nanoholes in gold films. *Langmuir* 20:4813-4815
13. Yeh WH, Petefish JW, Hillier AC (2011) Diffraction-based tracking of surface plasmon resonance enhanced transmission through a gold-coated grating. *Anal. Chem.* 83:6047-6053
14. Liu H, Lalanne, P (2008) Microscopic theory of the extraordinary optical transmission, *Nature* 728-731
15. Devaux E, Ebbesen, TW, Weeber JC, Dereux A (2003) Launching and decoupling surface plasmon via micro-grating. *Appl. Phys. Lett.* 83:4936-4938
16. Sheröter U, Heitmann, D. (1998) Surface-plasmon-enhanced transmission through metallic gratings. *Phys. Rev. B* 58:15419-15421
17. Kim T, Kim D, Lee J, Lee Y, Oh S (2008) Preparation of gold-silica heterogeneous nanocomposite particles by alcohol-reduction method. *Mater. Res. Bull.* 43:1126-1134
18. Kim J, Kim D, Veriansyah B, Kang JW, Kim JD (2009) Metal nanoparticles synthesis using supercritical alcohol. *Mater. Lett.* 63:1880-1882
19. Yang MH, Qu FL, Lu YS, Shen GL, Yu RQ (2008) In situ chemical reductive growth of platinum nanoparticles on glass slide for the mass fabrication of biosensors. *Talanta* 74:831-835
20. Hutter E, Fendler JH, Roy D (2001) Surface plasmon resonance studies of gold and silver nanoparticles linked to gold and silver substrates by 2-aminoethanethiol and 1,6-hexanedithiol. *J. Phys. Chem. B* 105:11159-11168
21. Lyon LA, Musick MD, Natan MJ (1998) Colloidal Au-enhanced surface plasmon resonance immunosensing. *Anal. Chem.* 70:5177-5183
22. Lyon LA, Peña DJ, Natan MJ (1999) Surface plasmon resonance of Au-colloid-modified Au films: particles sized dependence. *J. Phys. Chem. B* 103:5826-5831

23. Baba A, Kaneko F, Advincula RC (2000) Polyelectrolyte adsorption processes characterized in situ using the quartz crystal microbalance technique: alternate adsorption properties in ultrathin polymer films. *Colloids Surf. A* 173:39-49
24. Sriwichai S, Baba A, Deng S, Huang C, Phanichphant S, Advincula RC (2008) Nanostructured ultrathin films of alternating sexithiophenes and electropolymerizable polycarbazole precursor layers investigated by electrochemical-surface plasmon resonance (EC-SPR) spectroscopy. *Langmuir* 24:9017-9023
25. Baba A, Matsuzawa T, Sriwichai S, Ohdaira Y, Shinbo K, Kato K, Phanichphant S, Kaneko F (2010) Enhanced photocurrent generation in nanostructured chromophore/carbon nanotube hybrid layer-by-layer multilayers. *J. Phys. Chem. C* 114:14716-14721
26. Baba A, Kanetsuna Y, Sriwichai S, Ohdaira Y, Shinbo K, Kato K, Phanichphant S, Kaneko F (2010) Nanostructured carbon nanotubes/copper phthalocyanine hybrid multilayers prepared using layer-by-layer self-assembly approach. *Thin Solid Films* 518:2200-2205
27. Palik ED (1985) *Handbook of Optical Constants of Solids* (Academic Press).
28. Mulvaney P (1996) Surface plasmon spectroscopy of nanosize of metal particles. *Langmuir* 12:788-800
29. Yu F, Ahl S, Caminade AM, Majoral JP, Knoll W, Erlebacher J (2006) Simultaneous excitation of propagating and localized surface plasmon resonance in nanoporous gold membranes. *Anal. Chem.* 78:7346-7350
30. Ahl S, Cameron PJ, Liu J, Knoll W, Erlebacher J, Yu F (2008) A comparative plasmonic study of nanoporous and evaporated gold films. *Plasmonics* 3:13-20
31. Ito M, Nakamura F, Baba A, Tamada K, Ushijima H, Lau KHA, Manna A, Knoll W (2007) Enhancement of surface plasmon resonance signals by gold nanoparticles on high-density DNA microarrays. *J. Phys. Chem. C* 111:11653-11662
32. Jiang G, Baba A, Ikarashi H, Xu R, Locklin J, Kashif KR, Shinbo K, Kato K, Kaneko F, Advincula RC (2007) Signal enhancement and tuning of surface plasmon resonance in Au nanoparticles/polyelectrolytes ultrathin films. *J. Phys. Chem. C* 111:18687-18694
33. Raether H (1988) *Surface Plasmons on Smooth and Rough Surfaces and on Gratings*. Springer, Berlin

CHAPTER IV

Distance-Dependent Surface Plasmon Resonance Coupling between a Gold Grating Surface and Silver Nanoparticles

Chutiparn Lertvachirapaiboon^{1,2}, Akira Baba^{1*}, Sanong Ekgasit^{2*}, Chuchaat Thammacharoen², Kazunari Shinbo¹, Keizo Kato¹, and Futao Kaneko¹

¹ Graduate School of Science and Technology and Center for Transdisciplinary Research, Niigata University, 8050 Ikarashi 2-nocho, Nishi-ku, Niigata 950-2181, JAPAN.

² Sensor Research Unit, Department of Chemistry, Faculty of Science, Chulalongkorn University, 254 Phayathai Rd., Patumwan, Bangkok 10330, THAILAND.

This article was submitted to The Journal of Physical Chemistry C.

ABSTRACT

In this study, we achieved an enhancement of the transmission surface plasmon resonance (T-SPR) intensity by depositing silver nanoparticles (AgNPs) onto a gold grating substrate. The T-SPR spectrum of the gold grating substrate with AgNPs showed a strong and narrow SPR peak located between 650 and 800 nm; the maximum SPR excitation was observed at a 35° angle of incidence. We controlled the distance between the gold grating surface and the AgNPs by using layer-by-layer (LbL) ultrathin films of poly(diallyldimethylammonium chloride) (PDADMAC) and poly(sodium 4-styrenesulfonate) (PSS) to study the distance dependence of coupling effect between the AgNPs and the gold grating substrate. The distance-dependent T-SPR response of peak position and intensity showed distinctive changes when the intermediate layer was 10 bilayers (~17 nm) thick. The strongest coupling surface plasmon excitation between the AgNPs and the gold grating substrate was obtained at this layer spacing. Furthermore, we explored the potential of the developed system as a switchable pH sensor. The T-SPR spectrum sensitively changed as the pH switched from acidic (pH 2) to alkaline (pH 12) conditions by the swelling/shrinking of the poly(allylamine hydrochloride) (PAH)/PSS LbL film, respectively, which was deposited between the AgNPs and the gold grating surface.

INTRODUCTION

Surface plasmon polaritons are strong electromagnetic waves that propagate to a metal/dielectric interface.^{1,2} Because surface plasmon resonance (SPR) is highly sensitive to the nearby refractive index at a thin metal surface, it has been widely employed in a number of applications.³⁻⁷ Recently, transmission surface plasmon resonance (T-SPR) has become a topic of interest because a large electric field induces strong and narrow spectra in the visible to near-infrared region.⁸⁻²¹ T-SPR was first observed on gold nanohole arrays;⁸ later, this phenomenon was also observed on gold grating patterns.¹⁵⁻¹⁹ Moreover, a strong electric field at the gold grating surfaces was observed, and this field provided an enhanced transmission of the ± 1 diffraction order.²⁰ We studied the enhancement of T-SPR properties based on grating patterns of recordable digital versatile discs (DVD-Rs) coated with thin gold films because of the flexibility and simplicity of this technique and have utilized this enhancement in several applications, including biosensors and tunable T-SPR.^{21,22}

Recently, the extraordinary transmission of light through AgNPs has been reported.^{22,23} Wang, et al.²³ considered coupling and decoupling²⁵⁻²⁷ processes at ZnO/Ag and Ag/ZnO grating interfaces with Ag nanoislands. Surface plasmon (SP) excitation was confined at the ZnO/Ag and Ag/ZnO interfaces (near-field), and the SP was subsequently radiated as enhanced light transmission (far-field). Brenier²³ reported an enhancement of the transmission of light through a disordered assembly of AgNPs. The AgNPs grafted with perfluorodecanethiol were introduced onto a ZrO₂-coated silica substrate. The transmission light was more intense than that of the oxide substrate over a wide wavelength range of 300–680 nm. This phenomenon should reveal the interference of light in the AgNPs films in terms of transmission enhancement.

In addition to the SPR light transmission observed on a gold grating substrate, this phenomenon could be further enhanced by the introduction of metal nanoparticles onto a gold grating surface. Recently, we reported the enhancement of a T-SPR signal by the direct synthesis of gold nanoparticles on gold grating surfaces.²⁸ The metal nanoparticles facilitate the coupling/decoupling of SPs and may also excite SPs from the AgNPs and gold grating substrate. In this study, because the T-SPR intensity is much greater than the absorption of localized surface plasmon resonance (LSPR) excitation of AgNPs, we monitored the coupling effect of SPs via shifts in the T-SPR peak position and via the increase in the T-SPR intensity at a wavelength of ~740 nm. The distance-dependent SPR coupling between the gold grating surface and the AgNPs with various thicknesses of the intermediate layer was investigated. We controlled the thickness of the intermediate layers by the number of poly(diallyldimethylammonium chloride)/ poly(sodium 4-styrenesulfonate) (PDADMAC/PSS) ultrathin film layers to determine the optimum distance that provides the greatest coupling of electric field enhancement. We further studied the distance effect of electric field coupling by changing the distance between intermediate layers via the swelling/shrinking of a polyelectrolyte. The poly(allylamine hydrochloride) PAH polyelectrolyte was protonated and deprotonated under acidic and alkaline conditions, respectively.²⁹ This phenomenon could also be used to control the distance between the gold grating surface and AgNPs. Here we monitored the thickness adjustment induced by pH switching in real time by a time-dependent study at a fixed wavelength of 760 nm while the pH was adjusted between 2 and 12. Simultaneously, we also explored a gold grating with a [(PAH/PSS)₁₀ + (PAH/AgNPs)₅] substrate as a switchable pH sensor by monitoring the kinetic curve of the film while the pH was adjusted; the results showed a dramatic change in the T-SPR intensity. The results

obtained for the enhancement and control of the T-SPR signal should be useful for various applications, including sensors and active plasmonic devices.

EXPERIMENTAL

SYNTHESIS OF SILVER NANOPARTICLES

A chemical reduction method was used to synthesize AgNPs. Ten milliliters of 9.26×10^{-3} M silver nitrate, AgNO_3 (Sigma-Aldrich, Japan), was added to 40.0 mL molar equivalents of sodium borohydride, NaBH_4 (Sigma-Aldrich, Japan), under vigorous stirring. In the synthesis, 2.0% (w/v) soluble starch (Sigma-Aldrich, Japan) was used as an effective stabilizer.³⁰⁻³³ After the AgNO_3 solution was added to the NaBH_4 solution, the color of the solution changed to yellow. A UV–visible spectrometer (V-650 UV–visible spectroscopy, JASCO) was used to monitor the extinction spectrum of the synthesized AgNPs. A transmission electron microscope (H-7650 TEM, Hitachi) was used to analyze the size of AgNPs. (The results of the AgNPs characterization are provided in supporting information, Figure S1.)

LAYER-BY-LAYER ADSORPTION

The cleaned BK7 glass substrates were functionalized by submerging in toluene containing 0.1 wt% 3-aminopropyltriethoxysilane (APS) for 30 min. The APS layer was charged by immersion in dilute HCl solution for 5 s, and the LbL ultrathin film was then immediately prepared.⁷ In case of the gold grating film, an approximately 50-nm-thick gold film was deposited by vacuum evaporation onto a polycarbonate DVD-Rs (Taiyo Yuden) grating substrate (a 3-nm-thick layer of chromium was used as an adhesion layer). The grating pitch of the DVD-R substrates was 740 nm. For the functionalization of the gold grating surface, the grating substrate was immersed for 3 h in a 1 mM aqueous solution of 3-mercaptopropylsulfonic acid sodium salt (MPS) and then rinsed with deionized water before the LbL deposition of ultrathin films. PDADMAC (20 wt% in water, MW ~200,000–350,000, Sigma, Japan) and PSS (MW 70,000, Sigma, Japan) at concentrations of 1 mg/mL were used for the LbL adsorption in this investigation.^{34,35} For the deposition of LbL ultrathin films, the substrates were alternately immersed in PDADMAC and PSS solutions for 15 min each. They were rinsed with deionized water for 2 min between each deposition. The injection cycle was repeated to form 1, 5, 10, 15, 20, or 30 bilayers on the substrate surface. The thickness of the LbL ultrathin films was estimated by prism-coupling Kretschmann SPR

measurements, and the theoretical SPR reflectivity curves were fitted by a Fresnel equation algorithm (Winspall software package, version 2.20). The average thickness of each bilayer was ~ 1.7 nm (the results are shown in supporting information, Figure S2).

DEPOSITION OF SILVER NANOPARTICLES

After the LbL ultrathin films were fabricated on the substrates, the substrates were again positively charged with a 1 mg/mL PDADMAC solution for the deposition of negatively charged AgNPs. Thin films of 100 ppm AgNPs were deposited onto the substrate surfaces using the immersion technique for 15 min each. Moreover, to increase the density of the AgNPs, the substrates were alternately immersed in PDADMAC and AgNPs solutions five times.

T-SPR SPECTROSCOPY

T-SPR measurements were conducted with a homemade T-SPR system equipped with a fiber-optic spectrometer (HR 4000, Ocean Optics) and a white light source (LS-1 tungsten halogen, Ocean Optics). The substrates were mounted on a rotation stage. White light was passed through a linear polarizer, and the T-SPR signals of the prepared substrates were then detected by the fiber-optic spectrometer. In all measurements, only zero-order transmission was detected. Surface plasmons were excited at the metal grating–dielectric interface by the irradiation of white light at fixed angles of incidence. Figure 1 shows a schematic diagram of the sample structure. To obtain normalized spectra, we subtracted the raw spectrum of s-polarized light from that of p-polarized light.

PH-SWITCHABLE SWELLING/SHRINKING INVESTIGATED BY T-SPR SPECTROSCOPY

In this study, we further studied the effect of the intermediate layer thickness on the SPR coupling by the swelling/shrinking a polyelectrolyte layer; we also explored the potential use of these films as switchable pH sensors. PAH (MW 70,000, Sigma, Japan) at a concentration of 1 mg/mL was used as a positive polymer layer. The amino group on PAH could be protonated and deprotonated under acidic and alkaline conditions, respectively.^{5,29} The swelling/shrinking transition of PAH/PSS at 10 bilayers was attempted on a gold grating substrate (thickness ~ 50 nm) with AgNPs. To measure the switchability of the T-SPR response, we fixed the wavelength at 750 or 760 nm. A solution of nitric acid with a pH of 2

and a solution of sodium hydroxide with a pH of 12 were used to investigate pH switchability.

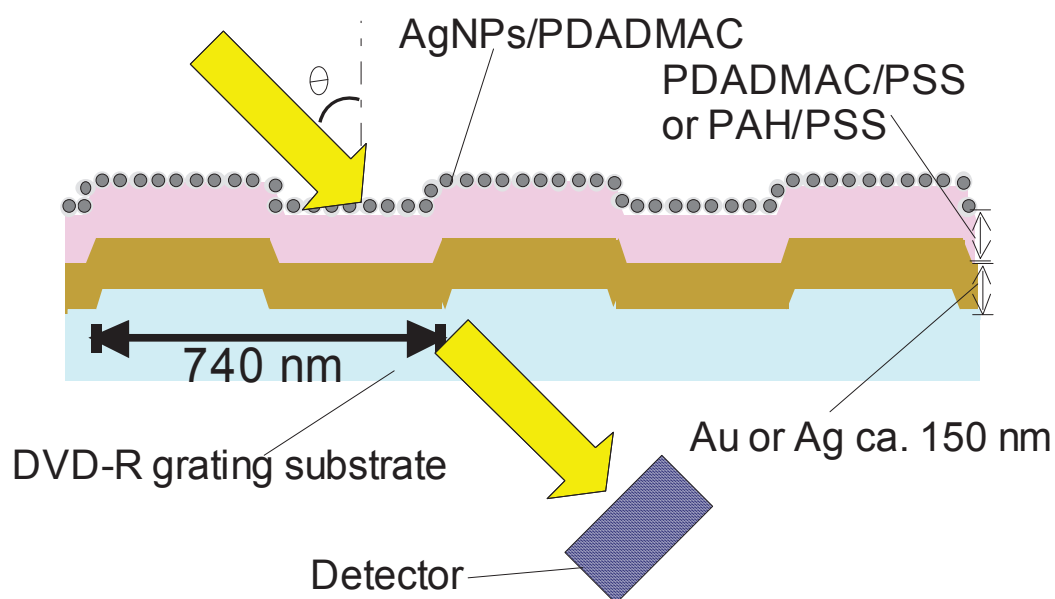


Figure 1 Schematic diagram of the sample structure.

RESULTS AND DISCUSSION

The deposition of five bilayers AgNPs/PDADMAC onto various thicknesses of PDADMAC/PSS intermediate layers on BK7 glass slides was studied by UV-vis absorption spectroscopy. As shown in Figure 2, AgNPs/PDADMAC was deposited onto the surface of a PDADMAC/PSS ultrathin film at the peak wavelength of 450 nm because of LSPR excitation.^{36,37} The extinction intensity of the AgNPs/PDADMAC layers on 10, 20, and 30 PDADMAC/PSS bilayer spacers was approximately the same, as were the peak positions in the spectra of all the samples. These results indicate that the amount of AgNPs on the substrate was similar. However, when the thickness of the intermediate layer was less than 10 bilayers, the extinction intensity of the AgNPs was lower than those of AgNPs in samples with thicker intermediate layers, especially in the cases of no bilayer (only PDADMAC) and 1 bilayer. These results indicate that a smaller amount of AgNPs were deposited onto the substrate surface because of a poorly charged or nonuniform surface of the intermediate layer.

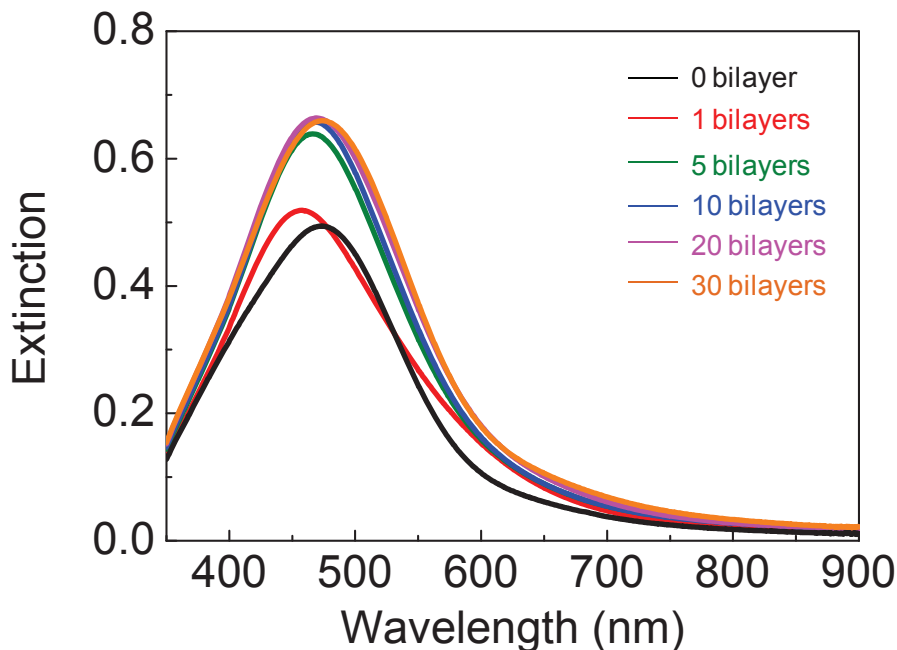


Figure 2 LSPR excitation of AgNPs at various distances from a BK7 glass slide.

We subsequently investigated the effect of AgNPs on the gold grating using grating-coupled T-SPR spectroscopy. The SPR phenomenon depends on the incident angle of light, excitation wavelength, diffraction grating pitch, diffraction order, dielectric constant of gold, and also dielectric constant of the environment.^{1,2} Figure 3a shows the T-SPR spectra of gold grating substrates in a water environment at an incident angle of 30°–40°. The intensities and peak positions in the T-SPR spectra were dependent on the angle of incidence. Under these conditions, the maximum T-SPR intensity should be observed at an incidence angle of 35°. An extraordinary transmission signal at this angle was observed at ~740 nm. This spectrum originated from the SPs at the interface between gold and water.²⁰ Figure 3b shows the T-SPR spectra of PDADMAC/PSS ultrathin films on gold grating substrates as a function of the number of bilayers at a 35° angle of incidence.

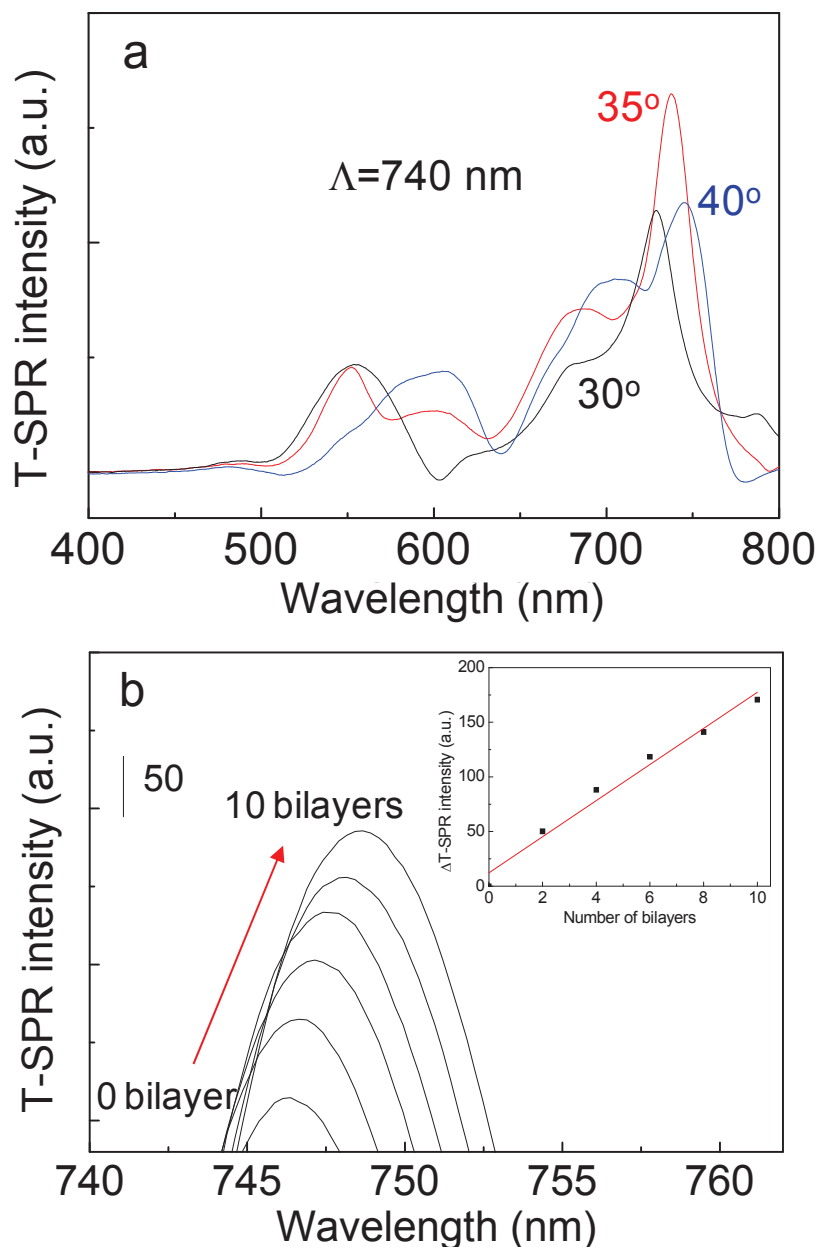


Figure 3 The T-SPR spectra of the gold grating substrate ($\Lambda = 740$ nm) at various angles (a). The T-SPR spectrum of an ultrathin film on the gold grating substrate was monitored at an incidence angle of 35° (b). The inset plot is the change in the T-SPR intensity as a function of the number of bilayers.

As shown in this figure, the narrow peak position at 746.5 nm in the spectrum of the gold grating substrate with MPS was observed. The T-SPR intensity increased, and the peak shifted toward longer wavelengths as the number of bilayers increased. The inset plot shows the linear increase in the maximum T-SPR intensity as a function of the number of bilayers.

The increase in the T-SPR intensity for 170.8 a.u. (from the gold grating substrate with MPS) was observed when the ultrathin film with 10 PDADMAC/PSS bilayers was deposited on the substrate surfaces. During the deposition of the ultrathin films, far-field transmitted SPs based on the coupling/decoupling SPs are facilitated by the ultrathin film on the gold grating surface due to the surface roughness of the film, which resulted in an increase in the T-SPR intensity upon LbL deposition. The T-SPR peak was shifted to longer wavelength (from 746.5 to 748.6 nm) after the deposition of the LbL ultrathin films. The T-SPR peak shift is related to changes in the effective dielectric constant at the interface of the gold film due to the adsorption of molecules on the surface.⁸⁻¹⁰ In this SP mode, the T-SPR peak always shifts toward a longer wavelength, and the peak intensity increases when an ultrathin film is deposited on a gold grating surface. The distance-dependent T-SPR between the gold grating surface and the AgNPs was studied by the deposition of PDADMAC/PSS ultrathin films as various numbers of bilayers on gold grating substrates, followed by the deposition of five bilayers of AgNPs/PSS on the PDADMAC/PSS film.

Figures 4a and b show T-SPR responses with 10 and 30 bilayers of the intermediate PDADMAC/PSS ultrathin films. After the PDADMAC/PSS LbL ultrathin films were deposited onto gold grating surfaces, the T-SPR spectra of substrates with 10 and 30 intermediate-layer bilayers showed peak positions at 745 and 750 nm, respectively. After AgNPs were deposited on their surfaces, increase in the T-SPR intensity and a red shift in the T-SPR spectrum were clearly observed. As shown in the figures, the change in intensity and the degree of red shift with 10 bilayers were clearly larger than those of 30 bilayers, whereas the amount of AgNPs adsorbed per PSS layer was approximately the same, as shown in Figure 2. Figure 4c shows a plot of the change in the T-SPR peak intensity (black line) and the peak-position shift (blue line) as functions of the number of bilayers of intermediate PDADMAC/PSS ultrathin films.

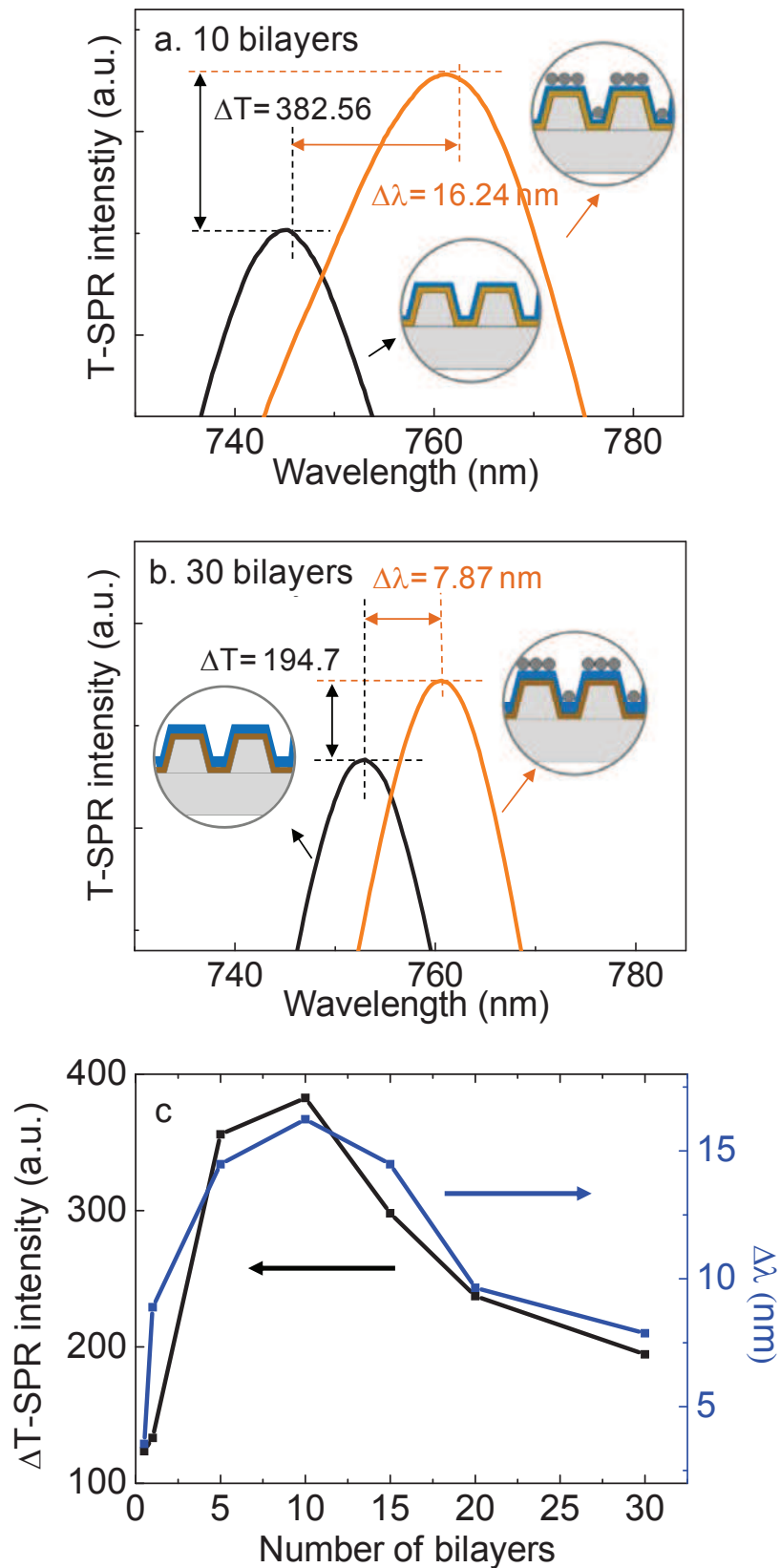


Figure 4 T-SPR spectra of films with 10-bilayer (a) and 30-bilayer (b) spacers, respectively. Plot of the T-SPR responses showing the shift in peak position and the increase in T-SPR intensity as a functions of the number of bilayers spacers (c).

As shown in this figure, the T-SPR peak intensity increased and shifted to longer wavelengths when the number of bilayers between the AgNPs and the metal surface was increased to 10 bilayers. When the number of bilayers was increased beyond 10 bilayers, a decrease in the T-SPR peak intensity and a smaller wavelength shift were observed. The maximum T-SPR intensity and the longest-wavelength peak position were observed with an intermediate layer of 10 bilayers (thickness ~ 17 nm). Under these conditions, the LSPR of the AgNPs near the surface of AgNPs should be excited. These SPs may interact with the propagating SP from the gold grating surface, which would lead to an enhancement of the far-field transmission signal.^{23,24} When the distance between the gold grating surface and the AgNPs is large, the interaction should be decreased. Thus, a decrease in the T-SPR enhancement was observed.

When the intermediate layer contained 0–5 bilayers, less T-SPR enhancement was observed. On the basis of the UV–vis spectra, the amount of AgNPs on 0- and 1-bilayer intermediate PDADMAC/PSS layers is approximately 75% of the amount on 10 bilayers, whereas the change in the T-SPR intensity with 0 bilayers is approximately 30% of the change observed with 10 bilayers. Hence, the diminished change in the T-SPR intensity is not caused only by the amount of AgNPs. This phenomenon can also be explained by photon scattering or near-field distribution on the substrate surface, which causes the weak coupling of surface plasmons. Figures 5a and b show the absorption spectra of AgNPs/PDADMAC as a function of the number of bilayers on a gold grating surface with an intermediate layer (10 bilayers of PDADMAC/PSS) and without an intermediate layer, respectively. The absorption spectrum of both systems was measured at an incidence angle of 35° under s-polarization; under these conditions, the propagating SP could not be excited. The inset spectra in Figure 5 show the corresponding T-SPR spectra with the p-polarization of incident light. As shown in Figure 5a, the absorption spectra of AgNPs on a gold grating substrate with an intermediate layer exhibited decreased absorbance in the longer-wavelength region, including 740 nm, upon AgNPs/PDADMAC deposition. This result indicates that an extraordinary transmission signal from this substrate can be obtained even without grating-coupled propagating SPE. Figure 5b shows the absorption spectra of AgNPs/PSS on a gold grating surface without an intermediate layer. In this case, the absorbance, including that at 740 nm, increased as the number of AgNPs/PDADMAC layers increased. This result indicates that an increase in the amount of AgNPs with the inclusion of an intermediate layer increased photon scattering or near-field distribution on the substrate.³⁸ Hence, the scattered light on the substrate surface

should enhance the decoupling of the transmission SP due to the altered wave vector of SPR. Thus, a remarkable increase in the T-SPR intensity was observed.

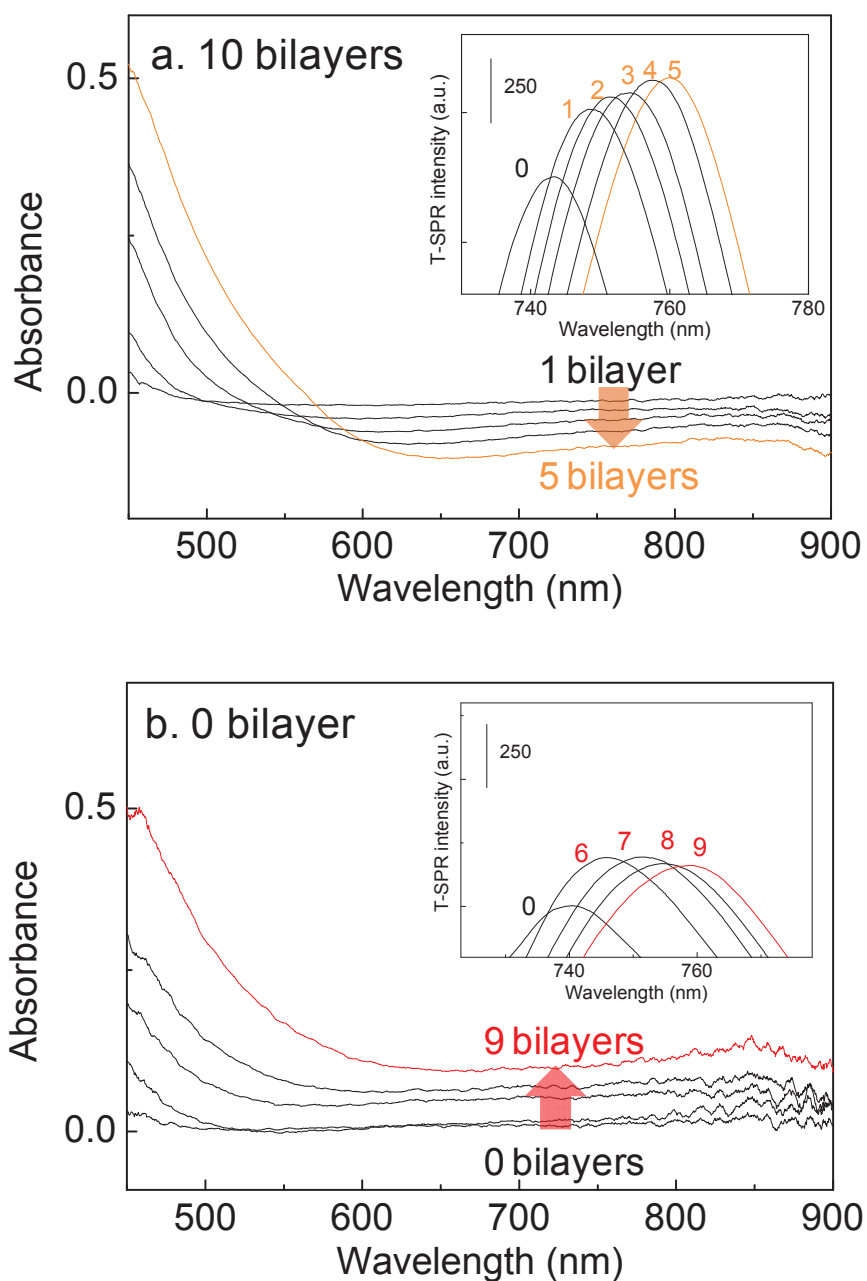


Figure 5 Absorption spectrum of AgNPs on a gold grating with an intermediate layer (10 bilayers of PDADMAC/PSS) (a) and without an intermediate layer (b) at an angle of incidence of 35° under s-polarization. The inset spectrum shows the development of the T-SPR spectrum when the number of AgNPs layers was increased.

The T-SPR intensity was highly sensitive to changes in the thickness of the intermediate layer. As previously discussed, when AgNPs were near the gold grating surface (i.e., when the intermediate layer contained fewer than 10 bilayers) or were distant from the surface (i.e., when the intermediate layer contained more than 10 bilayers), the excited surface plasmons at a wavelength of 740 nm were preferentially confined on the gold surface. This confinement resulted in the intensity of the transmission SPs at this wavelength decreasing to less than that observed when a thicker intermediate layer (10 bilayers) was used. To confirm distance-dependent SPR coupling, we fabricated a gold grating with a [(PAH/PSS)₁₀ + (PAH/AgNPs)₅] LbL film. Because the PAH layer can swell and shrink under acidic and alkaline conditions, respectively, the thickness of the intermediate layers of the system could be controlled by pH adjustments. Moreover, this substrate could be used as a switchable pH sensor. The pH-switchable behavior was investigated by the alternate injection of pH 2 and 12 solutions inside a T-SPR cell that was mounted on the holder at an incidence angle of 35°. Figure 6a shows the T-SPR spectra of a [(PAH/PSS)₁₀ + (PAH/AgNPs)₅] film at pH 2 (red line) and at pH 12 (blue line). At pH 2 (first cycle), the T-SPR intensity decreased to 58.1 a.u., and a blue shift in the T-SPR spectrum was observed (from 758 to 755 nm). On the basis of the results in Figure 4c, 10 bilayers of PAH/PSS intermediate film should result in the maximum T-SPR intensity. Hence, the decrease in intensity with the swelling of the PAH/PSS thin film is reasonable.

At pH 12, the T-SPR intensity still decreased further from that observed at pH 2 (79.0 a.u.), and an additional blue shift to 753 nm was observed in the T-SPR spectrum. Under alkaline conditions, PAH layers were deprotonated, and the electrostatic interactions between the PAH layers and the AgNPs were weakened.⁵ The shrinkage of the intermediate layer induced a decrease in the T-SPR intensity and a blue shift in the T-SPR spectrum as far-field transmission SPs became scattering photons on the substrate surface. As shown in Figure 4c, when the PAH/PSS film was shrunk to less than 8.5 nm (equivalent to the thickness of five bilayers of PDADMAC/PSS), the T-SPR intensity was less than that in the swollen state.

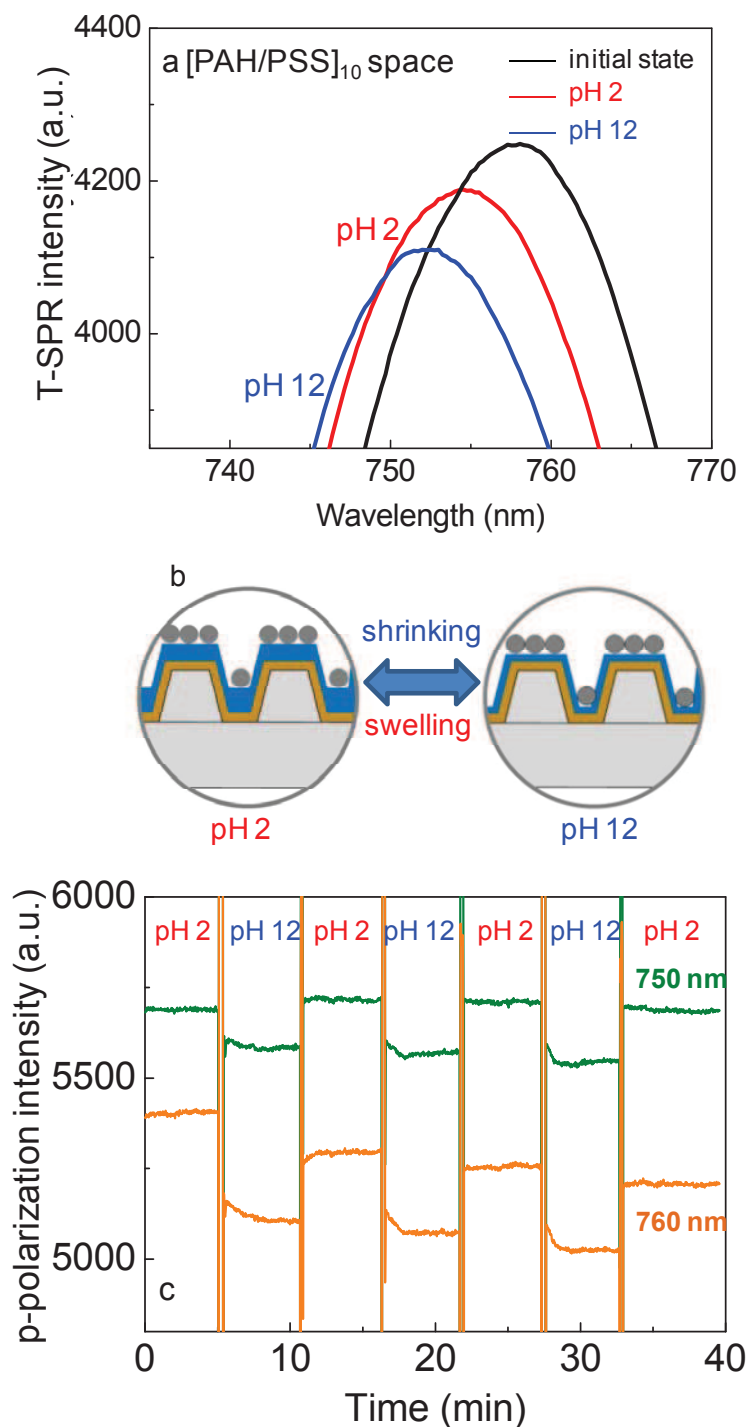


Figure 6 T-SPR spectrum of a [(PAH/PSS)₁₀ + (PAH/AgNPs)₅] film at pH 2 (red line) and at pH 12 (blue line) (a). Schematic diagram of swelling and shrinking as the PAH layers were protonated (pH 2) and deprotonated (pH 12), respectively (b). Kinetic curve of the film when the pH was switched between 2 and 12; the switch was repeated three times (c).

The kinetic curve of the film when the pH was switched between 2 and 12 is shown in Figure 6c. The different positions of the AgNPs on 10 bilayers of PAH/PSS provided the greatest change in the coupling of SPR by pH switching. At pH 2, the PAH layers were protonated, and an increase in the charge density could be observed by the swelling of the polyelectrolyte layers, which resulted in an increase in the p-polarization intensity. When the pH was switched from 2 to 12, the decrease in the p-polarization intensity at 760 nm was observed because of the shrinkage of the intermediate layer. Our substrates could be explored as switchable pH sensors, because a distinctive change in the T-SPR signal was obtained.

CONCLUSIONS

The enhancement of the T-SPR signal was obtained by controlling the position of AgNPs on polyelectrolyte intermediate ultrathin films on gold grating surfaces. An electric field enhancement from the AgNPs and gold grating substrate was obtained. The maximum coupling of the SP was observed at an intermediate layer thickness of ~17 nm. The distance dependence of the T-SPR response was confirmed by the observation of a swelling/shrinking effect of the controlled intermediate layer thickness. This study should be useful for the characterization of nanomaterials and for sensor applications.

REFERENCES

- (1) Knoll, W. *Annu. Rev. Phys. Chem.* **1998**, 49, 569-638.
- (2) Homola, J.; Koudela, I.; Yee, S. S. *Sens. Actuators B* **1999**, 54, 16-24.
- (3) Baba, A.; Aoki, N.; Shinbo, K.; Kato, K.; Kaneko, F. *ACS Appl. Mater. Interfaces* **2011**, 3, 2080-2084.
- (4) Baba, A.; Wakatsuki, K.; Shinbo, K.; Kato, K.; Kaneko, F. *J. Mater. Chem.* **2011**, 21, 16436-16441.
- (5) Jiang, G.; Baba, A.; Ikarashi, H.; Xu, R.; Locklin, J.; Kashif, K. R.; Shinbo, K.; Kato, K.; Kaneko, F.; Advincula, R. *J. Phys. Chem. C* **2007**, 111, 18687-18694.
- (6) Sriwichai, S.; Baba, A.; Deng, S.; Huang, C.; Phanichphant, S.; Advincula, R. C. *Langmuir* **2008**, 24, 9017-9023.
- (7) Baba, A.; Matsuzawa, T.; Sriwichai, S.; Ohdaira, Y.; Shinbo, K.; Kato, K.; Phanichphant S.; Kaneko, F. *J. Phys. Chem. C* **2010**, 114, 14716-14721.
- (8) Ebbesen, T. W.; Lezec, H. J.; Ghaemi, H. F.; Thio, T.; Wolff, P. A. *Nature* **1998** 391, 667-669.

- (9) Thio, T.; Ghaemi, H. F.; Lezec, H. J.; Wolff, P. A.; Ebbesen, T. W. *J. Opt. Soc. Am. B* **1999**, 16, 1743-1748.
- (10) Brolo, A.G.; Gordon, R.; Leathem, B.; Kavanagh, K. L. *Langmuir* **2004**, 20, 4813-4815
- (11) Wu, S.; Guo, P.; Huang, W.; Xiao, S.; Zhu, Y. *J. Phys. Chem. C* **2011**, 115, 15205-15209.
- (12) Im, H.; Sutherland, J. N.; Maynard, J. A., Oh, S. H. *Anal. Chem.* **2011**, 84, 1941-1947.
- (13) Blanchard-Dionne, A. P.; Guyot, L.; Patskovsky, S.; Gordon, R.; Meunier, M. *Opt. Express* **2011**, 16, 15041-15046.
- (14) Wu, L.; Bai, P.; Zhou, X.; Li, E. P. *IEEE Photon. J.* **2012**, 4, 26-33.
- (15) Xu, Z. C.; Dong, B.; Xue, J.; Yang, R.; Lu, B. R.; Deng, S.; Li, Z. F.; Lu, W.; Chen, Y.; Huq, E.; Qu, X. P.; Liu, R. *Microelectron. Eng.* **2010**, 87, 1297-1299.
- (16) Turker, B.; Guner, H.; Ayas, S.; Ekiz, O. O.; Acar, H.; Guler, M. O.; Dâna, A. *Lab Chip* **2010**, 11, 282-287.
- (17) Yeh, W. H.; Kleingartner, J.; Hillier, A. C. *Anal. Chem.* **2010**, 82, 4988-4993.
- (18) Singh, B. K.; Hillier, A. C. *Anal. Chem.* **2006**, 78, 2009-2018.
- (19) Singh, B. K.; Hillier, A. C. *Anal. Chem.* **2008**, 80, 3803-3810.
- (20) Yeh, W. H.; Petefish, J. W.; Hillier, A. C. *Anal. Chem.* **2011**, 83, 6047-605.
- (21) Janmanee, R.; Baba, A.; Phanichphant, S.; Sriwichai, S.; Shinbo, K.; Kato, K.; Kaneko, F. *ACS Appl. Mater. Interfaces* **2012**, 4, 4270-4275.
- (22) Baba, A.; Tada, K.; Janmanee, R.; Sriwichai, S.; Shinbo, K.; Kato, K.; Kaneko, F.; Phanichphant, S. *Adv. Funct. Mater.* **2012**, 22, 4383-4388.
- (23) Wang, P.; Zhang, D.; Kim, D. H.; Qiu, Z.; Gao, L.; Murakami, R.; Song, X. *J. Appl. Phys.* **2009**, 106, 103104-1-103104-5.
- (24) Brenier, R. *J. Phys. Chem. C* **2012**, 116, 5358-5366.
- (25) Liu, H.; Lalanne, P. *Nature* **2008**, 728-731.
- (26) Devaux, E.; Ebbesen, T.W.; Weeber, J. C.; Dereux, A. *Appl. Phys. Lett.* **2003**, 83, 4936-4938.
- (27) Shcröter, U.; Heitmann, D. *Phys. Rev. B* **1998**, 58, 15419-15421.
- (28) Lertvachirapaiboon, C.; Supunyabut, C.; Baba, A.; Ekgasit, S.; Thammacharoen, C.; Shinbo K.; Kato, K.; Kaneko, F. *Plasmonics*, DOI 10.1007/s11468-012-9400-2

- (29) De Geest, B. G.; Skirtach A. G.; De Beer, T. R. M.; Sukhorukov, G. B.; Bracke, L.; Baeyens, W. R. G.; Demeester, J.; De Smedt S. C. *Maccromol. Rapid Commun.* 2007, 28, 88-95.
- (30) Raveendran, P.; Fu, J.; Wallen, S. L. *J. Am. Chem. Soc.* **2003**, 125, 13940-13941.
- (31) Tongsakul, D.; Wongravee, K.; Thammacharoen, C.; Ekgasit, S. *Carbohydr. Res.* **2012**, 357, 90-97.
- (32) Singh, M.; Sinha, I.; Mandal, R. K. *Mater. Lett.* **2009**, 63, 425-427.
- (33) Shervani, Z.; Yamamoto, Y. *Carbohydr. Res.* **2011**, 346, 651-658.
- (34) Schlenoff, J. B.; Dubas, S. T. *Macromolecules* **2001**, 34, 592-598.
- (35) Ramos J. J. I.; Stahl, S.; Richter, R. P.; Moya, S. E.; *Macromolecules* **2010**, 43, 9063-9070.
- (36) Evanoff, D.D. Jr.; Chumanov, G. *J. Phys. Chem. B* **2004**, 108, 13957-13962.
- (37) Limsavarn, L.; Sritaveesinsub, V.; Dubas, S. T. *Mater. Lett.* **2007**, 61, 3048-3051.
- (38) Lumdee, C.; Toroghi, S.; Kik, P. G. *ACS Nano* **2012**, 6, 6301-6307.

CHAPTER V

CONCLUSIONS

Imprinting gold nanoparticles on a grating pattern was successfully developed. High-concentration gold nanoparticles were synthesized by chemical reduction method. Imprinting technique was used to fabricate gold grating film for use as a SPR sensor chip. The SPR signal from grating-coupling surface plasmon resonance and multimode surface plasmon resonance provided strong SPR excitation signals. This substrate was explored as a SPR sensor chip with respect to the sensitively shift upon the deposition of an organic thin film. This SPR substrate should be useful in photoelectric conversion and sensor applications.

The direct deposition of gold nanoparticles on gold grating substrate was fabricated by chemical reduction of gold salt with ethanol for use as a T-SPR substrate. The growth of gold was occurs in two phases. In the first phase, the total film thickness increases as the gold surface seeds AuNPs nucleation. In the second phase, the presence of AuNPs was occurred on the gold film surface and further growth to the larger particles. The AuNPs on the substrate surface increases the excitation of surface plasmons and facilitates decoupling at the back side of Au grating which corresponds well with the results of FDTD simulation. With respect to nano-rough surface and facilitation of decoupling, T-SPR sensitivity of gold grating substrate was improved by deposited AuNPs film on their gold surface. This hybrid SPR substrate could be used for the nanometer order characterization, ultrathin film characterization, surface binding analysis, and biosensor applications.

Moreover, SPR signal could be enhanced by deposition of silver nanoparticles on gold grating surface. An electric field enhancement from this hybrid material was also observed by T-SPR spectroscopy. The enhancement of the T-SPR signal was obtained by controlling the position of silver nanoparticles on polyelectrolyte intermediate ultrathin films on gold grating surfaces. The maximum coupling of the surface plasmon was observed at an intermediate layer thickness of ~ 17 nm. We explored the potential of the developed system as a switchable pH sensor applications using distinctive shift of T-SPR signal which was sensitivity to the distance between silver nanoparticles and gold grating surface.

SUGGESTIONS FOR FUTURE WORK

1. We have studied only spherical shape of gold and silver nanoparticles with specific size range. Synthesis gold and silver nanoparticles for other size and shape should be developed for further understanding in the relationship of localized and propagating surface plasmon resonance.
2. These hybrid T-SPR substrates should be explored in several applications such as biosensors, specific chemical trace analysis, and microfluidic systems.

APPENDICES

APPENDIX A

SUPPORTING INFORMATION FOR CHAPTER II

Solution-Based Fabrication of Gold Grating Film for Use as a Surface Plasmon Resonance Sensor Chip

Chutiparn Lertvachirapaiboon^{1,2}, Ryosuke Yamazaki¹, Prompong Pienpinijtham², Akira Baba^{1*}, Sanong Ekgasit^{2*}, Chuchaat Thammacharoen², Kazunari Shinbo¹, Keizo Kato¹, and Futao Kaneko¹

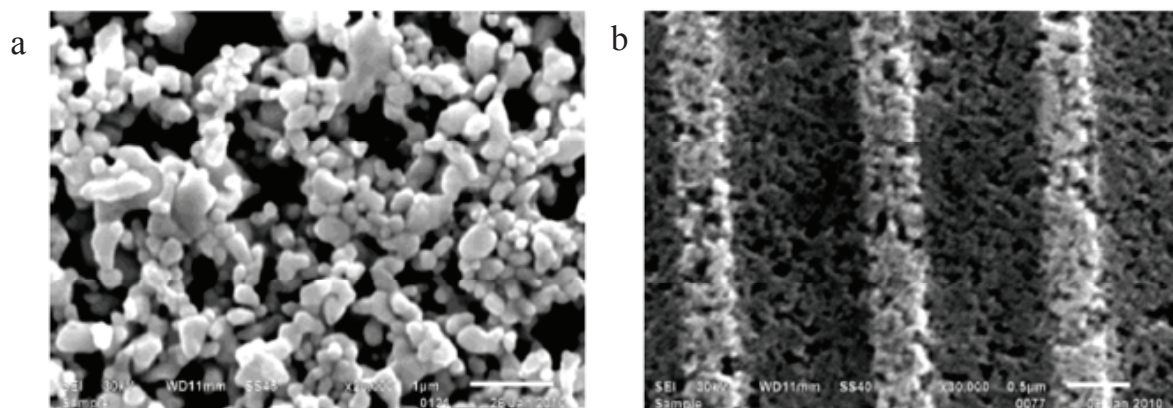


Figure S1 SEM images of AuNP imprinted on a grating surface using AuNP at concentrations of 10,000 ppm (starch 0.1% w/v) (a) and 5,000 ppm (starch 2.0% w/v) (b).

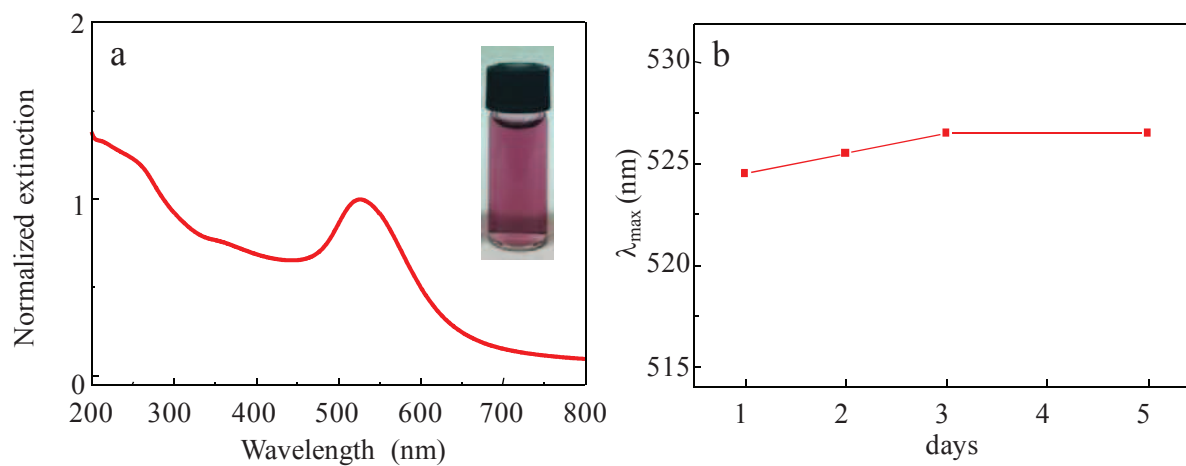


Figure S2 LSPR spectrum of AuNP (10 ppm) synthesized at the concentration of 5000 ppm (a) and LSPR peak position shift over 5 days (b).

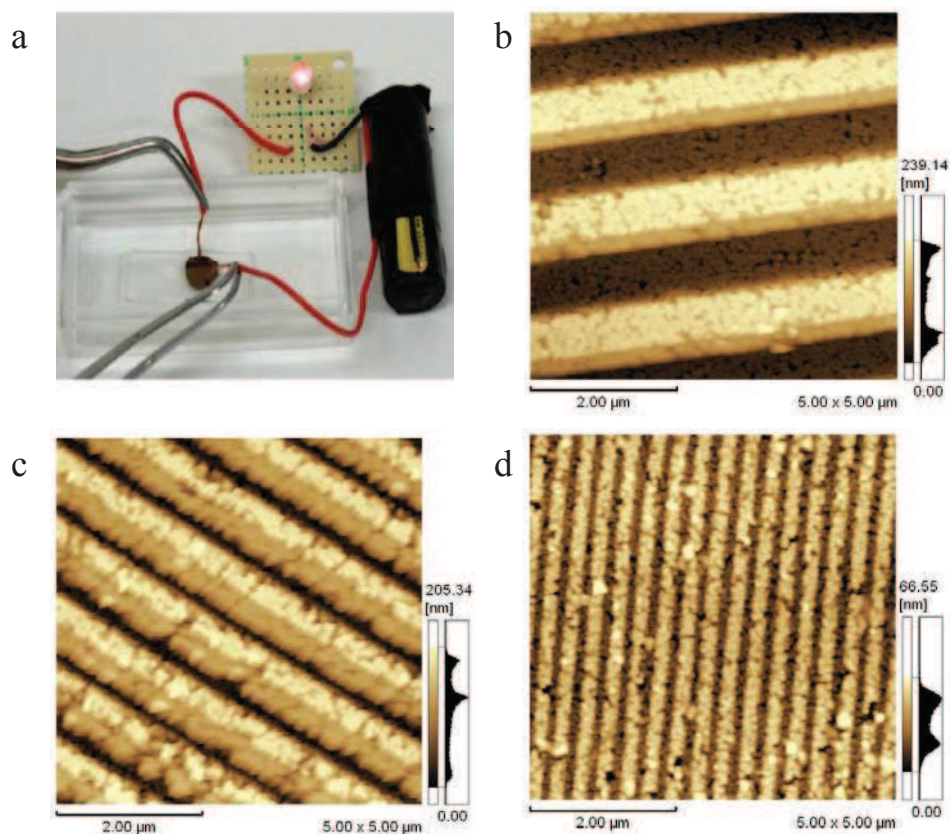


Figure S3 Photographic images of the conductivity of imprinted AuNP (a), the AFM images of imprinted AuNP of various grating patterns: CD-R (b), DVD-R (c) and BD-R (d).

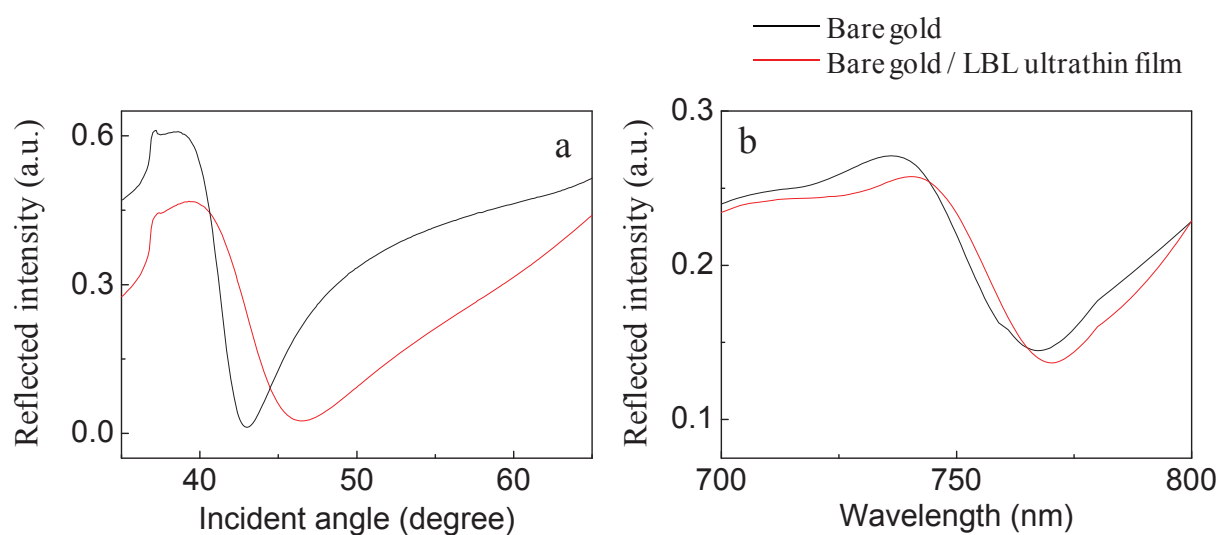


Figure S4 SPR angular curves of evaporated gold substrate before and after the deposition of ultrathin film obtained using a He-Ne laser (a) and white light excitation (b).

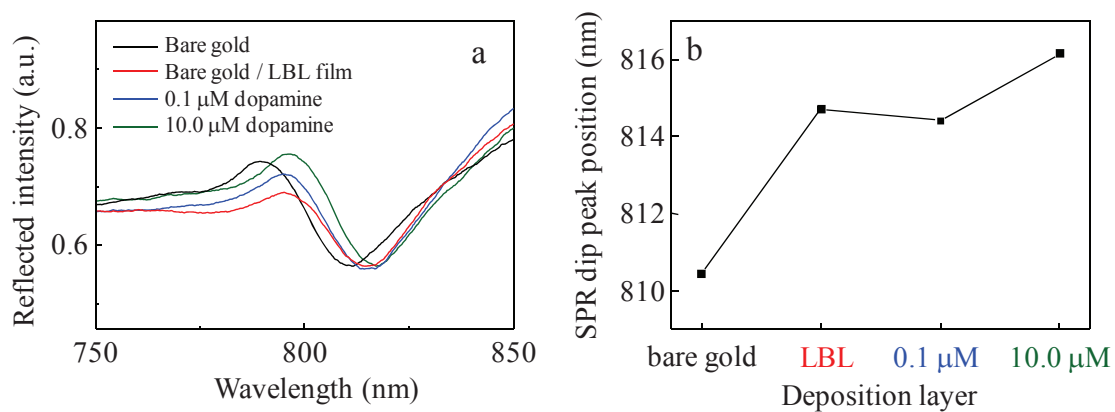


Figure S5 SPR spectra of a dopamine sensor of imprinted AuNP at a 60° angle of incidence; the SPR spectrum of bare gold (black line), after deposition of LBL ultrathin film (red line), and after deposition of dopamine at $0.1 \mu\text{M}$ (blue line) and $10.0 \mu\text{M}$ (green line) (a) and SPR dip peak position as a function of deposition layer (b).

APPENDIX B

SUPPORTING INFORMATION FOR CHAPTER III

Transmission Surface Plasmon Resonance Signal Enhancement via Growth of Gold Nanoparticles on a Gold Grating Surface

Chutiparn Lertvachirapaiboon^{1,2}, Chirayut Supunyabut², Akira Baba^{1*}, Sanong Ekgasit^{2*}, Chuchaat Thammacharoen², Kazunari Shinbo¹, Keizo Kato¹,
and Futao Kaneko¹

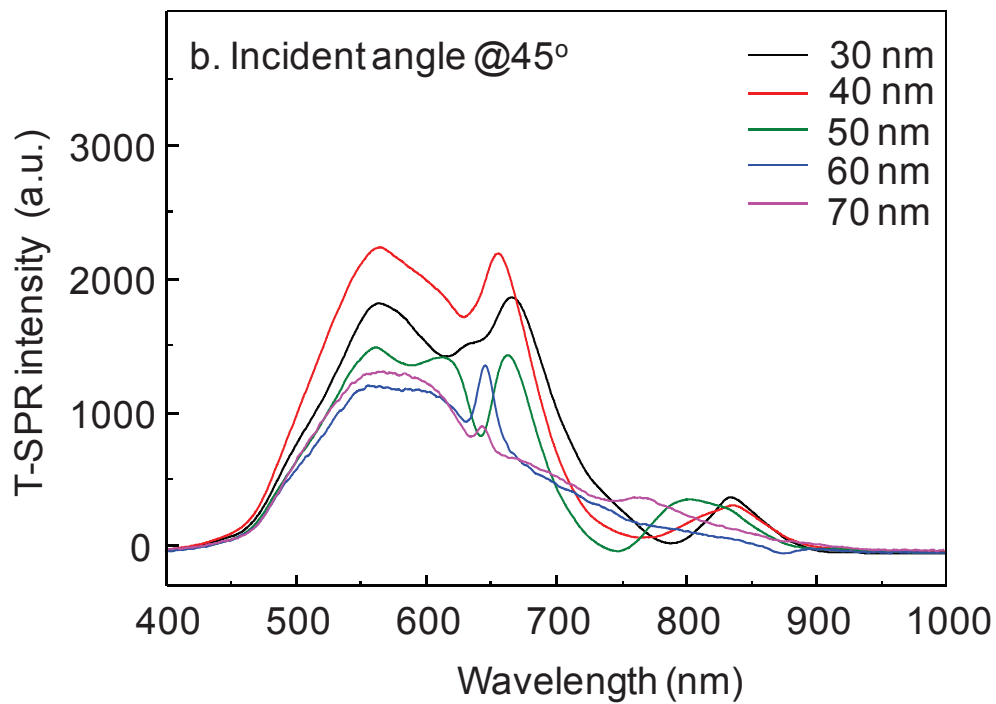


Figure S1 The T-SPR property in ambient air as a function of the thickness of gold film.

APPENDIX C

SUPPORTING INFORMATION FOR CHAPTER IV

Distance-Dependent Surface Plasmon Resonance Coupling between a Gold Grating Surface and Silver Nanoparticles

Chutiparn Lertvachirapaiboon^{1,2}, Akira Baba^{1*}, Sanong Ekgasit^{2*}, Chuchaat Thammacharoen², Kazunari Shinbo¹, Keizo Kato¹, and Futao Kaneko¹

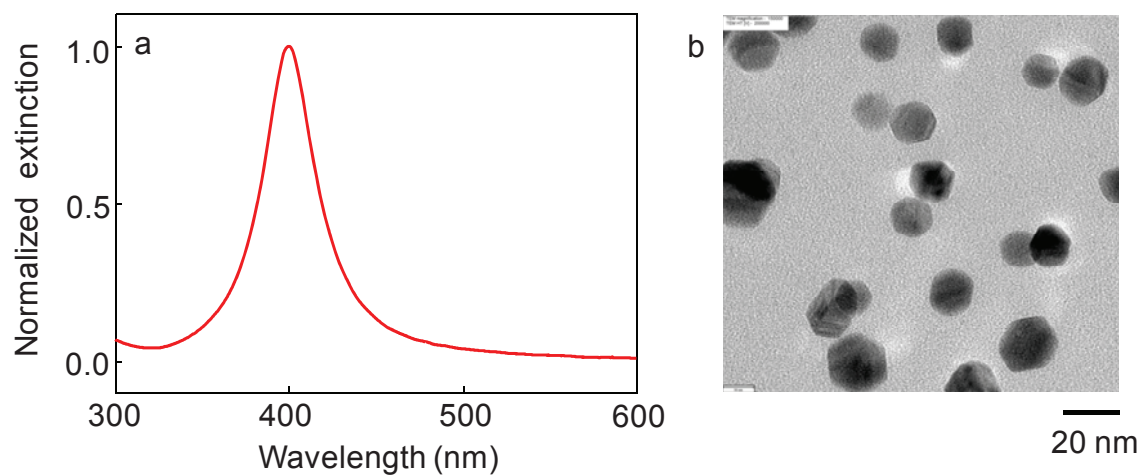


Figure S1 Normalized extinction spectrum of AgNPs (a) and a TEM image of the AgNPs (b).

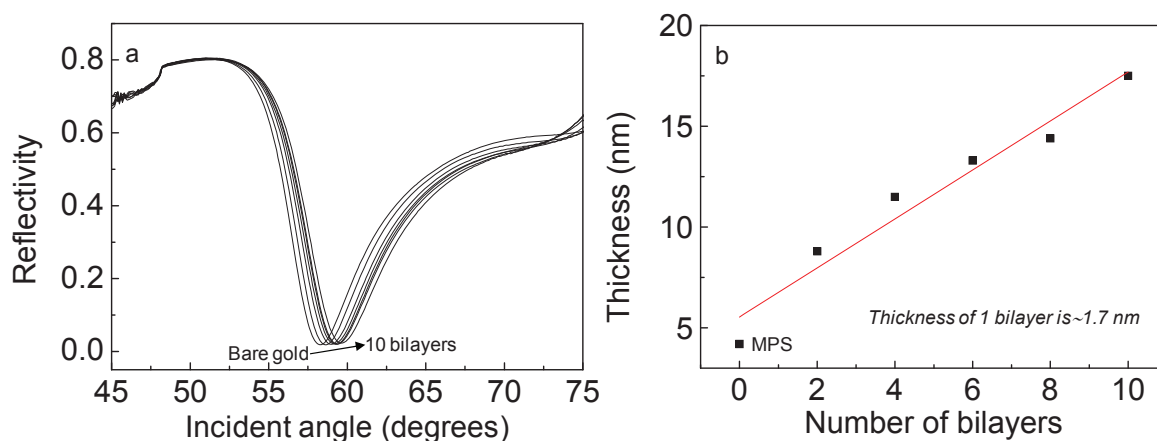


Figure S2 Shifts in the SPR angle of 10 PDADMAC/PSS bilayers on a gold film surface (a), which gives an average thickness of ~ 1.7 nm for each bilayer (b) under the assumption that the dielectric constant of the film is 1.920, which was obtained from the SPR simulation of a 10-bilayer film with a thickness of 17 nm.

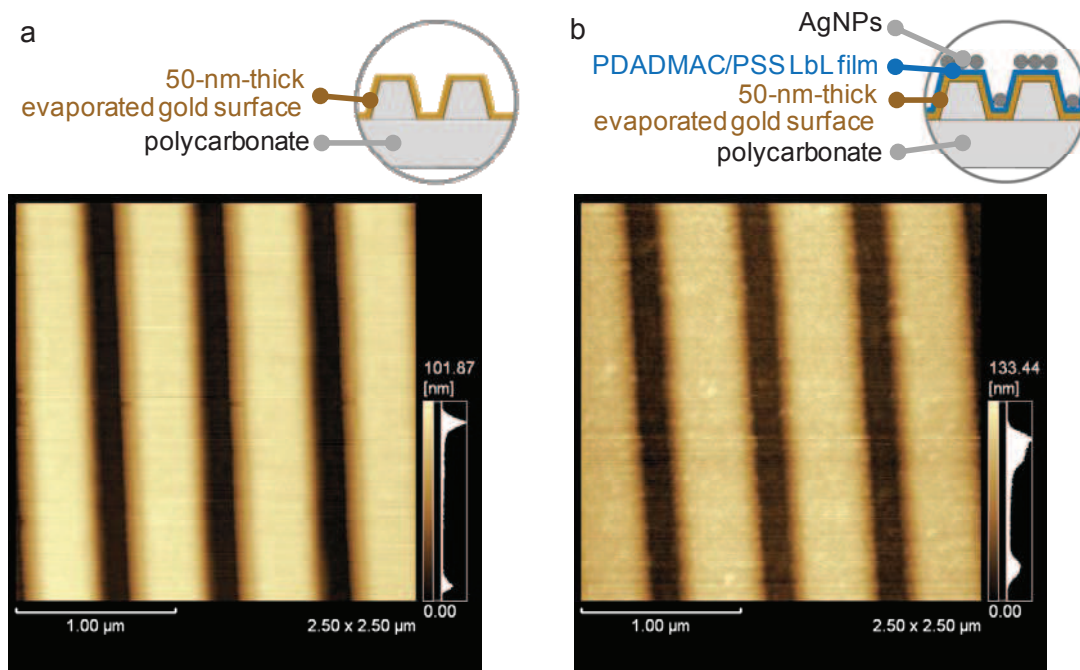


Figure S3 AFM images of a gold grating surface (a) and a gold grating with [(PDADMAC/PSS)₁₀+(PDADMAC/AgNPs)₅] (b).

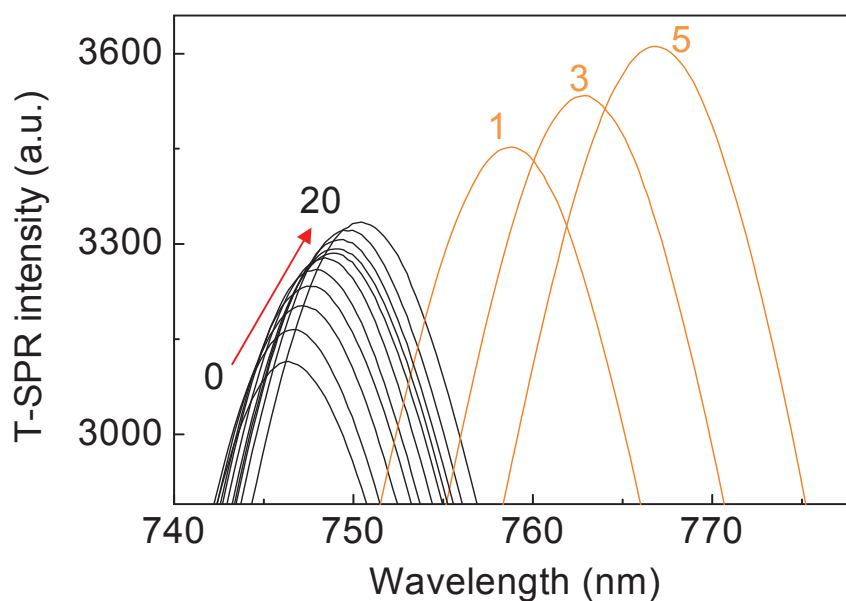


Figure S4 Evolution of the T-SPR spectrum of a PDADMAC/PSS LbL ultrathin film with 0 to 20 bilayers on a gold grating substrate was monitored at a 35° angle of incidence (black lines); the orange lines show the spectra after 1 to 5 bilayers of AgNPs were deposited on the ultrathin film.

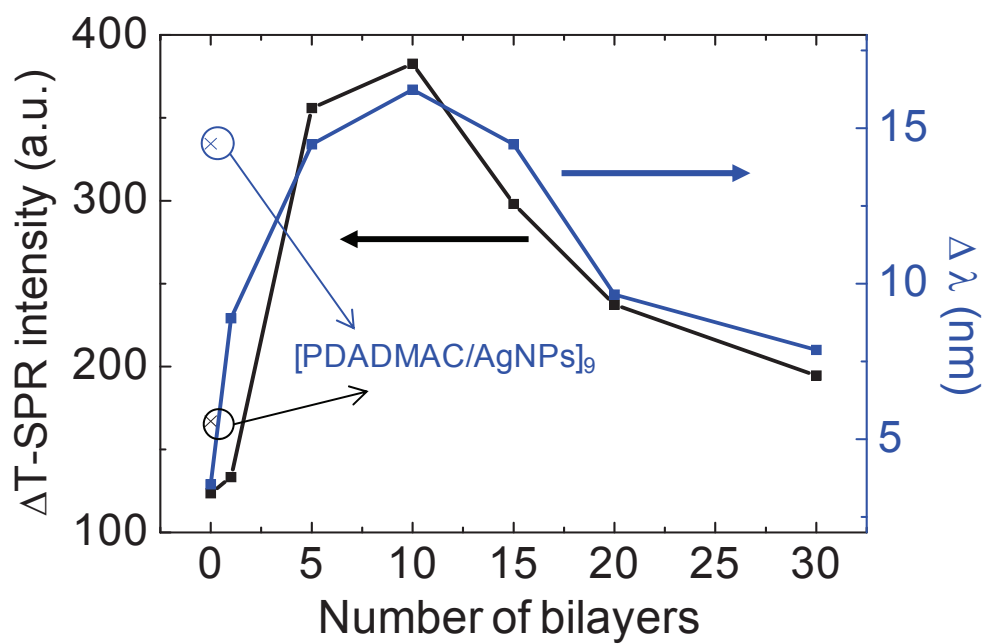


Figure S5 Plot of T-SPR responses showing the shift in the peak position and the increase in the T-SPR intensity as functions of the number of bilayer spacers.

APPENDIX D

A. CONFERENCES

1. **Global circus symposium**, 3 February 2011 at Niigata, JAPAN.
2. **IEICE Technical Report on Organic Material Electronics**, 8 July 2011 at Niigata, JAPAN.
3. **The 2011 International Symposium on Electrical Insulating Materials (ISEIM 2011)**, 6-10 September 2011 at Kyoto, JAPAN.
4. **The 2011 KJF International Conference on Organic Materials for Electronics and Photonics (KJF-ICOMEF 2011)**, 15-18 September 2011 at Gyeongju, KOREA.
5. **Technical Report on Organic Material Electronics**, 18-19 November 2011 at Kanazawa, JAPAN.
6. **Global circus symposium**, 3 February 2011 at Niigata, JAPAN.
7. **The First ASEAN Plus Three Graduate Research Congress (AGRC)**, 1-2 March 2012 at Chiangmai Thailand, THAILAND.
8. **The 2012 Annual Meeting of The Institute Electrical Engineer of Japan**, 20-23 March 2012 at Hiroshima, JAPAN.
9. **IEICE Technical Report on Organic Material Electronics**, 24 May 2012 at Tokyo, JAPAN.
10. **Small Science Symposium**, 10-12 December 2012 at Singapore, SINGAPORE.
11. **The 30th Annual Conference of the Microscopy Society of Thailand (MST30)**, 23-25 January 2013 at Chanthaburi, THAILAND.

B. AWARDS

- 2011 The Most Valuable Poster Presentation Award in terms of excellent presentation in Mutual Visiting type Poster (MVP) Session in 2011 International Symposium on Electrical Insulating Materials (ISEIM 2011).
- 2013 FIRST PRIZE Oral Presentation in Biological Science Session in The 30th Annual Conference of the Microscopy Society of Thailand (MST30).

C. PUBLICATIONS

1. **Lertvachirapaiboon, C.**, Yamazaki R., Pienpinijtham P., Baba A., Ekgasit S., Thammacharoen C., Shinbo K., Kato K., and Kaneko F. Solution-Based Fabrication of Gold Grating Film for Use as a Surface Plasmon Resonance Sensor Chip. Sensors and Actuators B: Chemical, 173 (2012) : 316-321.

2. Wongravee K., Parnklang T., Pienpinijtham P., **Lertvachirapaiboon C.**, Ozaki Y., Thammacharoen C., and Ekgasit S. Chemometric analysis of spectroscopic data on shape evolution of silver nanoparticles induced by hydrogen peroxide. Physical Chemistry Chemical Physics, 15 (2013) : 4183-4189.
3. **Lertvachirapaiboon, C.**, Supunyabut C., Baba A., Ekgasit S., Thammacharoen C., Shinbo K., Kato K., and Kaneko F. Transmission Surface Plasmon Resonance Signal Enhancement via Growth of Gold Nanoparticles on a Gold Grating Surface. Plasmonics, 8 (2013) : 369-375.
4. Parnklang T., **Lertvachirapaiboon C.**, Pienpinijtham P., Wongravee K., Thammacharoen C., and Ekgasit S. H₂O₂-triggered shape transformation of silver nanospheres to nanoprisms with controllable longitudinal LSPR wavelengths, RSC Advances, Accepted
5. **Lertvachirapaiboon C.**, Baba A., Ekgasit S., Thammacharoen C., Shinbo K., Kato K., and Kaneko F. Distance-Dependent Surface Plasmon Resonance Coupling between a Gold Grating Surface and Silver Nanoparticles. Journal of Physical chemistry C, Submitted.

VITAE

Name: Mr. Chutiparn Lertvachirapaiboon; **Date of Birth:** 28 December 1984

Address: 3/1102, Phaholyothin Rd. Bangkhen, Bangkok, 10220, THAILAND

E-mail: l_chutiparn@hotmail.com

Education:

- 2013 Ph.D. (Electrical and Electronic Engineering, Niigata University, JAPAN)
- 2009 Master of Science (Physical chemistry, Chulalongkorn University, THAILAND)
- 2007 Bachelor of Science (Chemistry, King Mongkut's University of Technology
Thonburi, THAILAND)

Scholarship:

The "Global Circus" Program of Niigata University supported by the Ministry of Education, Culture, Sports, Science and Technology, JAPAN.